Vol. 720: 95–116, 2023
https://doi.org/10.3354/meps14397

MARINE ECOLOGY PROGRESS SERIES
Mar Ecol Prog Ser

Published October 5

Infaunal community structure, diversity, and function in Pacific-Arctic shelf sediments: a comparison of meiofaunal- and macrofaunal-sized nematodes

Brittany R. Charrier[1,*], Jeroen Ingels[2], Seth L. Danielson[1], Sarah L. Mincks[1]

[1]College of Fisheries and Ocean Sciences, University of Alaska Fairbanks, Fairbanks, AK 99775, USA
[2]Coastal and Marine Laboratory, Florida State University, St Teresa, FL 32358, USA

ABSTRACT: Meiofauna, and nematodes in particular, perform essential roles in benthic ecosystems and serve as bioindicators of disturbance and environmental change. In the Pacific Arctic, a region experiencing rapid environmental change, this component of the fauna has received little attention, and the role of meiofauna in ecosystem processes is poorly understood. We collected multi-core samples at 10 stations in the northern Bering and southern Chukchi Seas in June 2018 and characterized the sedimentary environment. We also assessed meiofauna community structure and abundance at higher taxonomic levels and evaluated genus-level nematode composition in meiofaunal (63–500 µm) and macrofaunal (>500 µm) size fractions. Nematodes were classified by feeding type and life-history strategies. Total meiofauna abundance and biomass varied greatly, with 1449–12 875 ind. 10 cm^{-2} and 373–2325 µg dry weight 10 cm^{-2} for the upper 5 cm of sediment. Estimated production of meiofaunal-sized nematodes was 5–28 g C m^{-2} yr^{-1}. Four distinct communities of meiofaunal-sized nematodes were identified in different sub-regions reflecting food availability and substrate type. The meiofaunal- and macrofaunal-sized nematodes represented 2 distinct communities. The unique taxonomic composition and large standing stock of the macrofaunal-sized nematodes (22 ± 15% of total nematode biomass) suggest they are critical components of the infauna and merit further research to assess their role in critical ecosystem functions. This study provides the first genus-level characterization of nematodes and some of the first measurements of meiofauna standing stock in the region, contributing important data for assessing ecosystem function in a rapidly changing Arctic.

KEY WORDS: Nematoda · Meiofauna · Macrofauna · Functional traits · Trophic diversity · Pacific Arctic

1. INTRODUCTION

Meiofauna play critical roles in ecosystem functioning (reviewed by Schratzberger & Ingels 2018), including carbon and nutrient cycling (Coull 1999, Rysgaard et al. 2000, Bonaglia et al. 2014), linking microbial and upper-trophic levels of the food web (Gee 1989, Coull 1990, Kennedy 1994), and serving as bioindicators of environmental change (Ridall & Ingels 2021). Tight pelagic–benthic coupling on Arctic shelves supplies substantial inputs of phytodetritus to the benthos (Grebmeier & McRoy 1989, Grebmeier & Barry 1991) and has been correlated with abundant meiofauna communities (Górska et al. 2014). Important sources of organic matter (OM) include phytoplankton, ice algae, other sources of ice-derived OM such as bacteria and meiofauna (North et al. 2014, Mäkelä et al. 2018, Gradinger & Bluhm 2020),

*Corresponding author: brjones8@alaska.edu

Publisher: Inter-Research · www.int-res.com

and terrestrial material delivered via riverine input and coastal erosion (Belicka & Harvey 2009, Bell et al. 2016, Zinkann et al. 2021). This tight pelagic–benthic coupling also sustains high macrofaunal biomass on the Pacific-Arctic shelf (Grebmeier et al. 2015). However, the meiobenthos remains poorly studied and has been identified as a critical data gap in the region (Nelson et al. 2014, Lovvorn et al. 2016).

Only a handful of meiofaunal studies have been conducted in the Pacific Arctic. One study quantified the abundance and distribution of meiofauna in the Chukchi Sea (Lin et al. 2014) but only identified specimens to higher taxonomic levels (e.g. phylum and class). Community composition and functional diversity of nematodes were not resolved further, even though nematodes accounted for 96.6% of total meiofaunal abundance in the shallow shelf region. Meiofaunal abundance and biomass were quantified in the northeast Chukchi Sea (Hajduk 2015), and nematode community structure and function were assessed (Mincks et al. 2021). High variability in meiofaunal community structure and biomass was detected, driven by spatial and temporal environmental heterogeneity. These earlier studies pointed to a need to further explore functional diversity in the meiofauna, particularly in the context of rapid environmental change manifesting as unprecedented high temperatures and low sea-ice persistence (Grebmeier et al. 2018, Baker et al. 2020b, Huntington et al. 2020). A comprehensive assessment of regional patterns in the structure and function of benthic communities is essential to assess how benthos will respond to continuing changes in distinct Arctic marine settings.

Nematodes are generally the most abundant metazoan meiofaunal taxon in marine sediments. Functional traits are reasonably well described for nematode genera, especially feeding types and life-history strategies, which makes these traits easily comparable among studies (Wieser 1953, Bongers et al. 1991). Consequently, nematode communities are valuable in assessing ecosystem function (Yeates et al. 2009, Schratzberger & Ingels 2018) and provide insights into ecological and biogeochemical processes occurring in the benthic ecosystem, such as food availability, hydrodynamic conditions, and sediment biogeochemistry (e.g. Ingels et al. 2011b, Gunton et al. 2017, Román et al. 2018).

While nematodes are well known to reflect environmental conditions and ecosystem processes, macrofaunal-sized nematodes are often ignored in infaunal studies. Standardized sieve sizes operationally define meiofauna as individuals that pass through an upper mesh of 300–1000 µm and are retained on a lower 32–63 µm mesh (Giere 2009). The separation between these size fractions aligns with a trough in the bimodal size distribution of benthic infaunal metazoans, which corresponds to a shift in optimum life-history strategy from small meiofaunal organisms living interstitially within the sediment to large macrofaunal organisms capable of actively manipulating the sediment matrix (Warwick 1984). Thus, macrofaunal-sized nematodes are commonly excluded from meiofaunal studies due to their large size and ignored in macrofaunal studies because they are not considered macrofaunal taxa sensu stricto and require meiofaunal taxonomic expertise. However, these larger nematodes exhibit distinct assemblage structure and functional diversity relative to meiofaunal nematodes (Sharma et al. 2011, Baldrighi & Manini 2015) and can contribute substantially to macrofaunal abundance (Baldrighi & Manini 2015, Gunton et al. 2017).

Our overall goal was to improve understanding of benthic community structure and function on the Pacific-Arctic shelf by examining the little-studied meiofauna, with a primary focus on nematodes. We explored broad spatial patterns in total abundance and composition of meiofaunal communities in the context of environmental settings on the northern Bering and southern Chukchi Sea shelves. We then conducted a more detailed taxonomic and functional-group characterization of the meiofaunal- and macrofaunal-sized nematodes in surface sediments, including estimation of biomass, and tested relationships to environmental variables.

Previous analyses of macrofaunal and microbial communities in the same study area identified 4 distinct eco-regions (Charrier et al. 2023, Walker et al. 2023). Horizontal current speed was a key driver of these spatial patterns in the environment, with grain-size characteristics and OM deposition — the dominant influences on infaunal community structure in general — largely influenced by these currents. With relatively high OM levels across this shelf study area, we hypothesized that the meiofaunal community as a whole would show limited spatial variation, whereas nematode assemblages would reflect these 4 distinct hydrographic settings ranging from strong lateral advection (sandy, high current) to more quiescent depositional (muddy, low current) settings. Our sampling strategy was not designed to detect small-scale differences or heterogeneity, which we know exist in meiobenthos and nematode community patterns (Fonseca et al. 2010, Ingels & Vanreusel 2013); instead, detecting regional differences in faunal assemblages in conjunction with environmental con-

trasts was the objective. We also expected that taxonomic composition of the meio- and macrofaunal nematodes would be significantly different from each other, given that relatively few nematode genera have adult sizes that are large enough to belong to the macrofaunal size class, and macrofaunal nematode community composition has been found to be more similar between ocean basins than between meiofaunal- and macrofaunal-sized nematodes within a study area (Sharma et al. 2011). In addition, as macrofaunal-sized nematodes can comprise substantially more biomass per individual than meiofaunal-sized nematodes (Sharma et al. 2011), we wanted to assess the contribution of macrofaunal-sized nematodes to total macrofaunal standing stock and determine the role of this neglected group in benthic ecosystem function in shelf sediments. This study provides the first genus-level characterization and biomass estimates of nematodes in this region and highlights the need to conduct more detailed studies on the ecological roles of these taxa that will enhance investigations into climate change consequences in the Arctic.

2. MATERIALS AND METHODS

2.1. Study area and sampling

Samples were collected from the northern Bering and southern Chukchi Seas in June 2018 from the RV 'Sikuliaq' as part of the Arctic Shelf Growth, Advection, Respiration, and Deposition (ASGARD) project (Table 1, Fig. 1) that was funded under the umbrella of the Arctic Integrated Ecosystem Research Program (Arctic IERP; https://www.nprb.org/arctic-program; Baker et al. 2020a, 2023). This shallow shelf area is seasonally ice-covered and influenced by water masses with contrasting nutrient, temperature, and salinity characteristics. Cold, nutrient-rich Bering Shelf–Anadyr Water (BSAW) experiences mixing throughout the water column as currents accelerate through the Bering Strait constriction, which distributes nutrients that support high annual primary productivity in the region (Walsh et al. 1989, Danielson et al. 2017). As the BSAW fans out over the Chukchi Sea shelf, the current speed declines, resulting in elevated deposition rates of suspended particulate material to the seafloor (Grebmeier et al. 2015). In contrast, the warm, nutrient-poor Alaskan Coastal Water is generally located to the east and characterized by lower productivity and high terrestrial input (Danielson et al. 2017).

Table 1. Meiofauna metrics for each station sampled in 2018, including cluster group; sampling location; water depth (m); abundance (ind. 10 cm^{-2}) and biomass (µg DW 10 cm^{-2}) of total meiofauna and meio- and macrofaunal-sized nematodes in the upper 5 cm of sediment; and abundance (ind. 10 cm^{-2}), wet weight, dry weight, carbon weight (µg 10 cm^{-2}), and average individual size (µg DW $ind.^{-1}$) of meio- and macrofaunal-sized nematodes in the upper 1 cm of sediment. Groups are based on hierarchical agglomerative clustering and similarity profile test (SIMPROF; Fig. 3). DW: dry weight; WW: wet weight

Station	Group	Lat. (°N)	Long. (°W)	Depth (m)	63–500 µm							>500 µm					
					Meio. abund.	0–5 cm Nem. abund	0–5 cm Nem. biomass	0–1 cm – Nematodes Abund. ind.	0–1 cm – Nematodes WW	0–1 cm – Nematodes DW	0–1 cm – Nematodes Carbon weight	0–1 cm – Nematodes Avg. ind. DW	0–5 cm Nem. abund.	0–5 cm Nem. biomass	0–1 cm – Nematodes Abund. ind.	0–1 cm – Nematodes WW	0–1 cm – Nematodes DW	0–1 cm – Nematodes Carbon weight	0–1 cm – Nematodes Avg. ind. DW
DBO2.2	A	64.68	169.10	46	3860	3378	610	1977	1429	357	177	0.18	16	127	7	234	58	29	8
DBO2.4	A	64.96	169.89	48	3719	1840	862	985	1848	462	229	0.47	80	547	9	247	62	31	7
CNL3	B	66.50	168.96	56	1449	1278	418	192	251	63	31	0.33	30	70	4	41	10	5	2
CNL5	C	67.00	168.96	48	3035	2748	561	160	131	33	16	0.20	49	182	1	13	3	2	4
DBO3.6	C	67.90	168.24	58	7712	7268	2325	598	766	191	95	0.32	102	767	14	411	103	51	8
DBO3.8	C	67.67	168.96	51	6906	6775	1265	922	688	172	85	0.19	110	251	4	33	8	4	2
CL1	D	68.95	166.91	46	4135	3876	769	1450	1151	288	143	0.20	19	102	3	59	15	7	5
CL3	D	69.03	168.89	53	12875	12457	769	6920	2958	739	367	0.11	37	87	1	7	2	1	2
DBO3.3	D	68.19	167.31	48	1663	1542	373	647	626	157	78	0.24	47	461	22	861	215	107	10
IL4	D	67.40	165.84	39	5247	4589	1535	1501	2008	502	249	0.33	46	255	9	202	50	25	6

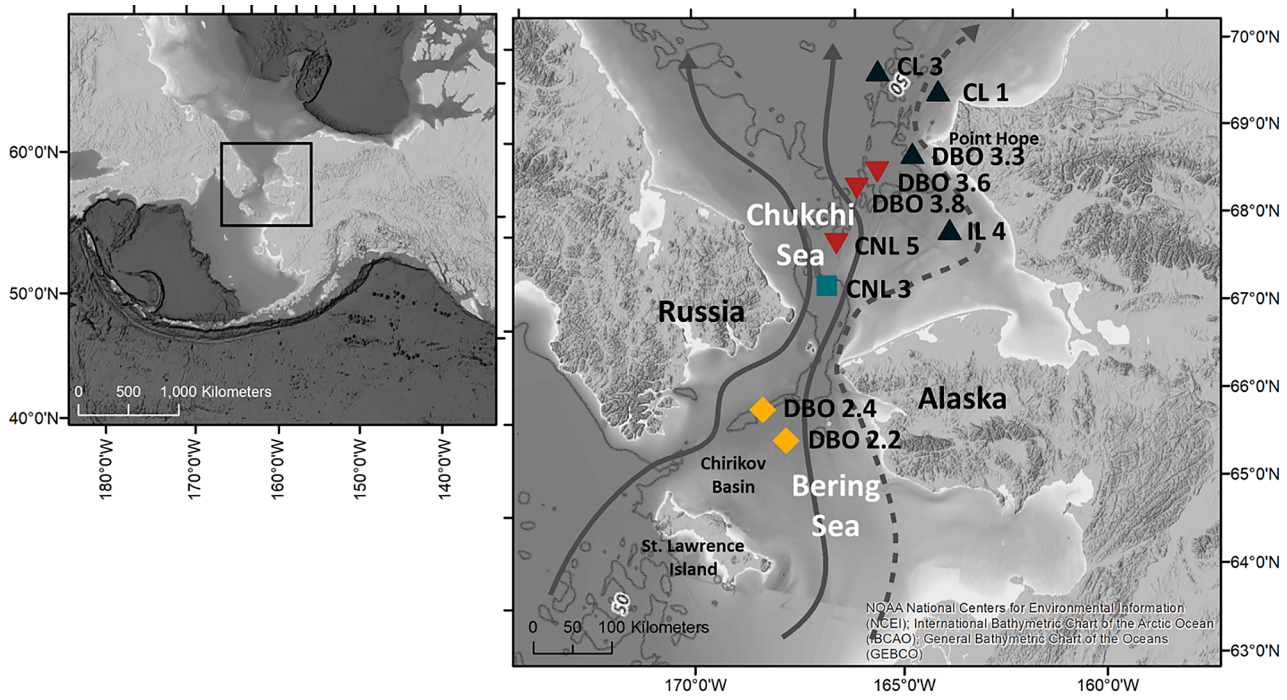

Fig. 1. Ten sampling locations in the northern Bering and southern Chukchi Seas in 2018. Symbols based on hierarchical agglomerative clustering of 63–500 µm nematode communities from Fig. 3. Group A = yellow diamonds; Group B = blue square; Group C = red inverted triangles; Group D = black triangles. Northward-moving currents include the Bering Shelf–Anadyr Water (solid grey lines) and the Alaska Coastal Water (dotted grey line)

Intact sediment cores with undisturbed surfaces were retrieved from 10 stations using an MC-800 multi-corer with 10 cm internal diameter tubes (Ocean Instruments). Sampling stations ranged from 39 to 58 m water depth (Table 1). One core from each station was selected for meiofauna sampling due to logistical and funding constraints on fieldwork and sample processing. Although small-scale spatial heterogeneity of the meiofaunal community cannot be assessed with this design, our efforts were focused on obtaining greater regional coverage to assess large-scale spatial variability. This sampling design does, however, have limitations with respect to assessing variability across all spatial scales, particularly with most of the region still markedly under-sampled. The cores were sectioned into 1 cm depth intervals down to 5 cm and preserved in 10% buffered formalin.

2.2. Meiofauna analysis

Meiofauna were separated from the preserved sediment samples using a decantation method (Creer et al. 2010), which has been used in other Arctic meiofaunal studies (Mincks et al. 2021). Samples were washed over a 63 µm sieve, transferred to 70% isopropanol, and stained with Rose Bengal. Prior to sorting, an upper sieve with a 500 µm mesh size was used to separate macrofaunal- (>500 µm) from meiofaunal-sized (63–500 µm) specimens. The lower sieve size of 63 µm is consistent with studies of shallow water and other habitats (Grove et al. 2006, Sajan et al. 2010), previous work in the nearby northeast Chukchi and Beaufort Seas (Mincks et al. 2021), and reference works on specific meiofauna methods (cf. Somerfield & Warwick 1996, 2013, Giere 2009). For the macrofaunal size fraction, all nematodes were counted for each sediment depth (0–5 cm), and the first 120 nematodes were picked from the surface layer only (0–1 cm) for further taxonomic identification and biomass estimation. All nematodes were identified if there were fewer than 120 individuals.

The 63–500 µm samples were split using a Wet Sample Divider (WSD-10, McLane Research Laboratories), and 10% of each sediment layer was processed for abundance of metazoan meiofauna identified to higher taxonomic levels (i.e. phylum, class; Higgins & Theil 1988, Giere 2009). As with the larger size fraction, nematode taxonomy was examined only for surface sediment layers (0–1 cm), with 100–150 nematodes randomly selected for genus-level identification and biomass estimation using a random num-

ber table and a gridded petri dish. This number of individuals generally reflects the composition of the whole nematode community (Soetaert & Heip 1990), allowing for greater efficiency in taxonomic analysis.

The selected meiofaunal- (N = 1124) and macrofaunal-sized (N = 483) nematodes were transferred to anhydrous glycerin using a glycerol–isopropanol–water solution and evaporated overnight in a drying oven at 50°C (Seinhorst 1959). Nematodes were then mounted on glass slides and identified to genus under a compound microscope using pictorial keys (Platt & Warwick 1988) and the Nemys database (Bezerra et al. 2021). Genus-level identification is sufficient in detecting ecological patterns (Somerfield & Clarke 1995), which was the primary goal of this study. Specimens that could not be identified to genus level were assigned to family.

Length and width of each mounted nematode were measured using a compound microscope and imaging software. Nematode wet weight (µg) was calculated using the equation $(L \times W^2)/(1.5 \times 10^6)$, where L is length (µm), and W is the maximum body diameter (µm). This equation is adapted from Andrassy (1956), assuming a specific gravity of 1.13 g cm^{-3} for marine nematodes (Ingels et al. 2013, Pape et al. 2013). Wet weight was converted to dry weight using a dry-to-wet weight ratio of 0.25 (Heip et al. 1985) and to carbon weight using a carbon-to-wet weight ratio of 0.124 (Jensen 1984).

Nematode functional traits were characterized in terms of feeding type and life-history strategy. The feeding type of each nematode was assigned based on buccal cavity morphology as classified by Wieser (1953): selective deposit feeders (1A), non-selective deposit feeders (1B), epistratum feeders (2A), and predators/scavengers or omnivores (2B). Each nematode was also assigned a life-history strategy based on c–p scores on a scale ranging from 1 (colonizers with short generation times and rapid reproductive rates) to 5 (persisters with long generation times and slow reproductive rates), based on Bongers (1990) and Bongers et al. (1991, 1995).

2.3. Environmental variables

Bottom-water temperature (°C) and salinity (practical salinity scale) data were collected using the Sea-Bird 9/11 CTD system onboard RV 'Sikuliaq', calibrated by the manufacturer, manually screened for spikes and other errors, and averaged into 1-decibar bins. Calibrated Sea-Bird CTD temperature and salinity sensor data are typically better than ±0.01 in accuracy and ±0.001 in precision. Average near-bottom water temperature of sampling stations was 1.15 ± 0.93°C (ranging from −0.6 to 2.4°C), and average near-bottom water salinity was 32.5 ± 0.3 (ranging from 31.9 to 33.0).

Sediment cores were collected from multi-core deployments at each station to analyze sediment grain-size characteristics (N = 1 core) and OM content (N = 3 cores; except at DBO2.4, N = 2 cores). Briefly, grain size analysis was conducted using a subsample of the upper 5 cm of sediment. Samples were suspended in dispersant and then separated into size fractions using a combination of wet and dry sieving. The <63 µm (silt/clay) fraction was treated with 30% hydrogen peroxide to remove OM prior to final weighing. Mean phi was calculated with the 'Grain Size Distribution and Statistics' (GRADISTAT v.8.0) package (Blott & Pye 2001, Blott 2010). Percent silt/clay, percent sand, and porosity (water content:total sediment wet weight) were included in data analysis. See Charrier et al. (2023) for further details.

OM was measured as chloropigment content, total organic carbon (TOC), total nitrogen (TN), and carbon to nitrogen (C:N) ratio. Stable carbon isotope signatures were also measured as an indication of carbon source. For these analyses, cores were sectioned in 0–1, 1–2, 2–3, 3–4, 4–5, 5–7, and 7–10 cm layers. Chloropigments were extracted in 100% acetone and analyzed as in Charrier et al. (2023) using a TD-700 fluorometer (Turner Designs). Fluorescence was converted to concentration units based on a standard curve (adapted from Arar & Collins 1997) produced using a chlorophyll *a* (chl *a*) standard (spinach extract C5753, Sigma-Aldrich). Each sediment sample was extracted twice, and the amount of chlorophyll yielded from each extraction was summed. Sediment chlorophyll parameters measured included chl *a*, phaeopigment (phaeo), and chloroplastic pigment equivalent (CPE; chl *a* + phaeo) inventories (µg cm^{-2}), and chl *a*: phaeo ratio.

Stable carbon isotope signatures ($\delta^{13}C$), TOC (mg cm^{-2}), and TN (mg cm^{-2}) were analyzed at the Alaska Stable Isotope Facility at the University of Alaska Fairbanks Water & Environmental Research Center. Stable isotope data were obtained by continuous-flow isotope ratio mass spectrometry, utilizing a Thermo Scientific Flash 2000 elemental analyzer and Thermo Scientific Conflo IV interfaced with a Thermo Scientific DeltaV Plus Mass Spectrometer. Stable isotope ratios were reported in δ notation as parts per thousand (‰) deviation from the international standard Vienna Pee Dee belemnite (carbon). Typically, instrument precision is <0.2‰.

The Pan-Arctic Regional Ocean Modeling System (PAROMS) 3-D sea ice and ocean circulation model was used to hindcast ocean current speed. PAROMS is configured with a horizontal resolution of about 5 km in our study region and 50 layers vertically through the water column. For complete model descriptions and data–model comparisons, see Curchitser et al. (2018) and Danielson et al. (2020). Based on a PAROMS hindcast integration of the year 2011, we computed summary statistics of the ocean current flow field across the study region: the mean and standard deviation of the instantaneous current speeds ($m\ s^{-1}$) over the upper 50 m of the water column (or to the seafloor where shallower) based on hourly snapshots of the flow field.

2.4. Data analysis

Multivariate analyses of community structure were conducted in PRIMER v7 (Clarke & Gorley 2015) with the PERMANOVA+ add-on (Anderson et al. 2008). Bray-Curtis similarity matrices were calculated on $\log(x+1)$ transformed data and displayed on non-metric multi-dimensional scaling (nMDS) plots to visualize similarities among samples. Samples with similar taxonomic composition were identified using hierarchical agglomerative clustering with group-average linking. A similarity profile (SIMPROF) procedure was used to delineate statistically significant groupings. Similarity percentage (SIMPER) analyses were conducted to identify genera contributing most to similarities within and dissimilarities between station groupings.

Relationships between meiofaunal-sized nematode community structure, environmental variables, and surface layer sediment variables were examined using a distance-based linear model (DistLM) with a stepwise selection criterion based on adjusted R^2, followed by distance-based redundancy analysis (dbRDA). After examining histograms, current speed was log-transformed. All environmental data were normalized. Variables were removed prior to the analysis due to multicollinearity determined by Pearson's correlation coefficients (>0.8), including mean phi, percent sand, porosity, chl *a*, TOC, and C:N. Variables allowed in model selection included depth, temperature, salinity, current speed, percent silt/clay, and surface sediment layer CPE, chl *a*:phaeo, phaeo, TN, and $\delta^{13}C$.

The RELATE routine was used to calculate a Spearman rank correlation coefficient between the Bray-Curtis similarity matrices for meiofaunal- and macrofaunal-sized nematode communities. Similarity matrices were constructed using $\log(x+1)$-transformed relative abundance data, because the abundances of the 2 size fractions differed by orders of magnitude. Analysis of similarities (ANOSIM) was performed to test for differences in community composition between the 2 size fractions.

Univariate descriptors of nematode diversity were calculated in PRIMER. Hill's numbers (H_0, H_1, H_2, and H_∞; Hill 1973, Heip et al. 1998), Pielou's evenness (J'), Shannon-Wiener diversity index (H'), and expected number of genera for 51 individuals (EG(51)) were calculated. The trophic diversity index (TDI) was calculated as the reciprocal of the trophic index (Heip et al. 1998):

$$\mathrm{TDI} = \left(\sum_{i=1}^{n} {q_i}^2\right)^{-1} \quad (1)$$

where q_i is the proportion of feeding type i in the assemblage, and n is the number of feeding types (Ingels & Vanreusel 2013). The maturity index (MI) was calculated as the sum of the products of the relative proportion of each genus and their c–p score (Bongers 1990, Bongers et al. 1991, 1995):

$$\mathrm{MI} = \sum_{i=1}^{n} v_i \times p_i \quad (2)$$

where v_i is the c–p score, and p_i is the relative proportion of genus i in the sample (Ingels & Vanreusel 2013).

3. RESULTS

3.1. Metazoan meiofauna

Total meiofaunal abundance (63–500 µm) was 1.7 to 8.9 times higher at the most northern station (CL3) than at the other stations, due mainly to a large abundance of small nematodes in the surface layer of sediment (Table 1, Fig. 2; Table S1 in Supplement 1 at www.int-res.com/articles/suppl/m720p095_supp1.xlsx). Two offshore stations in the southeast Chukchi Sea (DBO3.6 and DBO3.8) also had high meiofaunal abundance (Table 1, Fig. 2). The lowest abundances occurred at the stations immediately north of the Bering Strait (CNL3 and CNL5) and off the coast of Point Hope (DBO3.3), which had high current speeds.

Nematodes were the most abundant taxon at all stations and accounted for an average of 88% of total meiofaunal abundance (ranging from 49% at DBO2.4 to 98% at DBO3.8; Fig. 2; Table S1). Nauplii (6%) were the second most abundant group, followed by

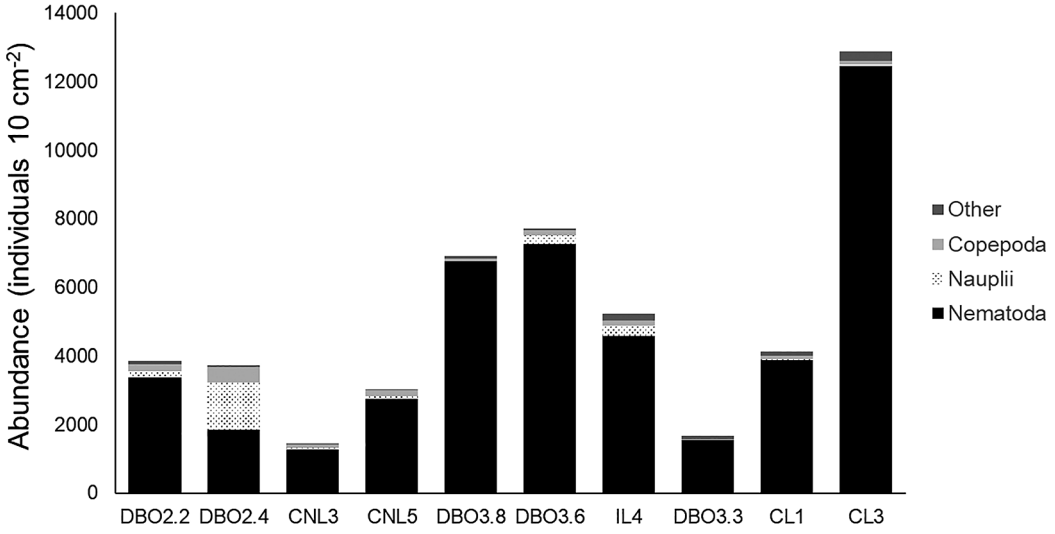

Fig. 2. Meiofaunal abundance (ind. 10 cm^{-2}) in the upper 5 cm of sediment at sampling locations on the northern Bering and southern Chukchi Sea continental shelves in 2018

copepods (4 %), bivalves (0.6 %), kinorhynchs (0.4 %), polychaetes (0.4 %), and ostracods (0.4 %). Kinorhynchs were only found at the 4 coastal Chukchi Sea stations (CL1, CL3, DBO3.3, and IL4), while ostracods were only found at the 2 central Chukchi Sea stations (DBO3.6 and DBO3.8). Nauplii abundance at DBO2.4 was 4.8 to 1073 times higher than at the other stations (Fig. 2; Table S1). Despite the differences in composition between stations, no significant spatial pattern was observed for higher-taxa community structure of meiofauna (π = 0.98, p = 0.22).

3.2. Meiofaunal-sized nematodes (63–500 µm)

Nematode community composition in the upper 1 cm of sediment significantly differed among 4 groups of stations (SIMPROF p = 0.05). Group A included stations south of the Bering Strait (DBO 2.2 and 2.4); CNL 3 immediately north of the Strait was distinct and formed Group B; Group C was composed of 3 southern Chukchi Sea stations (CNL 5, DBO 3.6, and DBO 3.8); and Group D contained the coastal Chukchi Sea stations (CL 1, CL 3, DBO 3.3, and IL 4; Figs. 1 & 3).

Although station groupings were based on nematode composition in the upper 1 cm of sediment, nematode abundance patterns down the vertical sediment profiles also differed noticeably between the groups. In Groups A and D, maximum abundance occurred at the sediment surface and rapidly declined with depth, whereas subsurface peaks in abundance were observed for Groups B and C (Fig. 4). Consequently, the surface (0–1 cm) abundance and average biomass were highest in Groups A and D and low for Groups B and C (Fig. 5). The very high average abundance in Group D was heavily influenced by Station

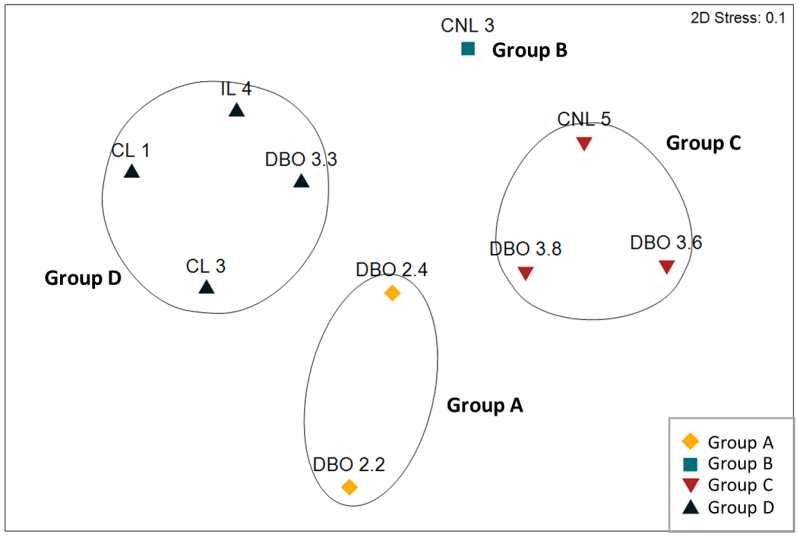

Fig. 3. Non-metric multi-dimensional scaling (nMDS) ordination for community structure of meiofaunal-sized (63–500 µm) nematodes in surface (0–1 cm) sediments based on abundance data (ind. 10 cm^{-2}). Ordination based on hierarchical agglomerative clustering with group-averaged linkage on log(x + 1) transformed data and Bray-Curtis similarity. Four significant station groupings, circled in black or as a singleton station, are based on the similarity profile test

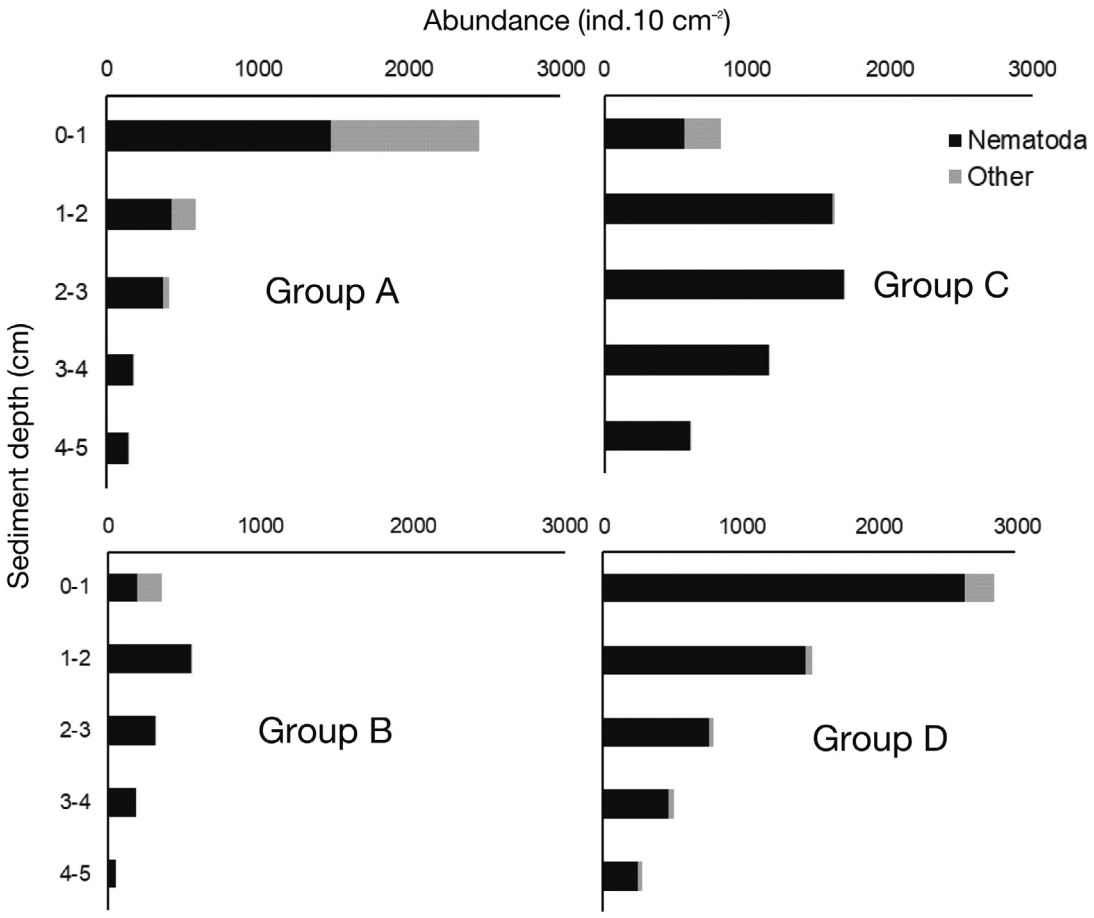

Fig. 4. Abundance (ind. 10 cm^{-2}) of nematodes (63–500 µm; black) and other meiofauna (gray) for each sediment depth and group. Groups are based on hierarchical agglomerative clustering and a similarity profile test (SIMPROF; Fig. 3)

(Stn) CL3 (~7000 ind. 10 cm^{-2} in the surface layer). This group was also dominated by small-sized nematodes, resulting in average biomass values similar to Group A despite the substantial difference in abundance.

Within-group similarity in community structure was driven not only by dominant taxa but also by less abundant genera (Table 2, Fig. 6; Table S2). Some genera were highly abundant across multiple station groups. For instance, *Daptonema* was 1 of the top 2 most abundant genera in Groups A, B, and C (Table 2). In Group C, genera that contributed most to within-group similarity were *Daptonema*, *Sabatieria*, and *Paramonohystera* (Table S2). *Daptonema* and *Paramonohystera* also contributed to within-group similarity in Group A, along with *Neochromadora* and *Oncholaimus*. Within-group similarity in Group D was mainly attributed to *Paramonohystera*, *Terschellingia*, *Tricoma*, and *Microlaimus*. Group B only contained 1 station, so a SIMPER analysis could not be performed for this group.

The dominant feeding types in Groups A, B, and C were non-selective deposit feeders (1B), e.g. the Xyalidae family (including *Daptonema* and *Paramonohystera*) and *Sabatieria* (Table 3). These non-selective deposit feeders were particularly abundant in Group C, accounting for nearly 80% of total abundance. On the other hand, the muddier coastal sites of Group D were dominated by selective deposit feeders (1A), including genera such as *Halalaimus*, *Tricoma,* and *Terschellingia*. The relative abundance of predators/scavengers (2B), e.g. *Oncholaimus* and *Viscosia*, was generally low (<3%), except in Group A, where almost 20% of individuals fell in this category. Group A exhibited the highest trophic diversity, with individuals more evenly distributed among feeding types (Table 3). Interestingly, taxonomic diversity in Group A was comparable to the other groups, demonstrating the importance of assessing both taxonomic and functional diversity.

General opportunists (c–p score = 2) were dominant in all groups (Table 3), particularly in Groups B (66.3%; e.g. *Sabatieria*, *Daptonema*, *Paramonohystera*) and C (80.7%; e.g. *Daptonema* and *Paramonohystera*), which had the lowest maturity indices.

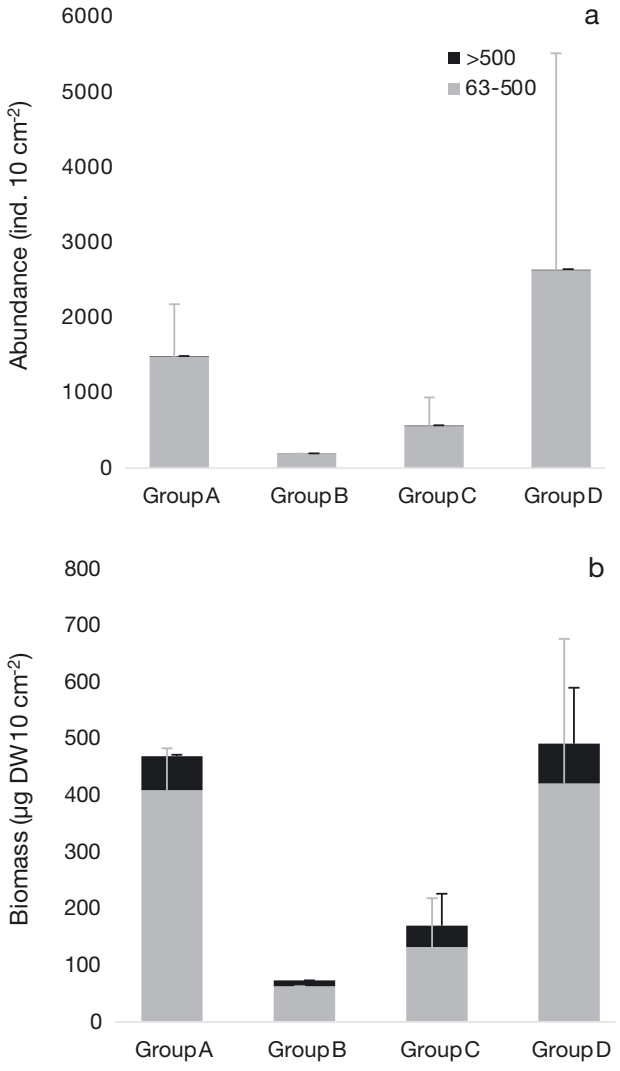

Fig. 5. Average ± SD meiofaunal- and macrofaunal-sized nematode (a) abundance (ind. 10 cm^{-2}) and (b) biomass (µg DW 10 cm^{-2}) in surface sediments (0–1 cm) for each group. Groups are based on hierarchical agglomerative clustering and a similarity profile test (Fig. 3)

Higher maturity indices in Groups A and D reflected a relatively large number of persisters (>20%; c–p score = 4), e.g. *Halalaimus* and *Tricoma*, compared to Groups B and C (<7%). Relative abundances of nematode genera and functional traits for each station are presented in Tables S3 & S4, respectively.

3.3. Environmental correlates of meiofaunal nematode assemblages

The selected DistLM model for meiofaunal-sized nematode communities in surface sediments accounted for 96.97% of total variation in community structure and included $\delta^{13}C$, chl *a*:phaeo, current speed, percent silt/clay, salinity, depth, TN, and phaeo (Fig. 7; Table S5). Key environmental parameters are summarized per group in Fig. 8, while environmental data for each station are presented in Table S6. Selection of $\delta^{13}C$, chl *a*:phaeo, and TN in the model suggest the freshness of OM was an important correlate of nematode community structure in this region. Some of the selected environmental predictors were highly correlated (Pearson's correlation coefficients >0.8) with other parameters excluded from the analysis. The parameter $\delta^{13}C$ was correlated with C:N, chl *a*:phaeo with chl *a*, TN with TOC, and percent silt/clay with mean phi, percent sand, porosity, and TOC.

The first dbRDA axis was most positively correlated with chl *a*:phaeo and negatively correlated with salinity and depth. Groups C and D separated along this axis, with higher chl *a*:phaeo, lower salinity, and muddier sediments in Group D (Fig. 7). Groups A and B fell between Groups C and D along the first axis, but with a clear separation between Group A and the other groups along the second axis, which was positively correlated with $\delta^{13}C$ and negatively correlated with salinity and TN. Group A was mainly distinguished by higher $\delta^{13}C$ values, sandier sediment, and lower TN. The third axis was highly correlated with chl *a*:phaeo and current speed, with Stns CNL3 and DBO3.3 distinguished by high current speeds and chl *a*:phaeo.

3.4. Macrofaunal-sized nematodes (>500 µm)

Macrofaunal-sized nematodes contributed a small amount to total nematode abundance in the upper 5 cm of sediment (1.6 ± 1.2%; 16 to 110 ind. 10 cm^{-2}), but a considerable amount to total nematode biomass (22 ± 15%; Fig. 5), ranging from 6% at CL3 to 55% at DBO3.3. Macrofaunal-sized nematode community structure showed no significant spatial pattern (π = 1.7, p = 0.65; Fig. S1 in Supplement 2 at www.int-res.com/articles/suppl/m720p095_supp2.pdf), so was not used to assess spatial heterogeneity on a regional scale or in terms of correlation to environmental characteristics. Macrofaunal-sized nematode community structure was distinct from that of the meiofaunal-sized nematodes (ANOSIM R = 0.36, p = 0.0002; Fig. 9). However, spatial patterns in taxonomic composition between meiofaunal- and macrofaunal-sized nematodes were significantly related (RELATE test: rho = 0.37, p = 0.0095), indicating that while taxonomic composition differed between the 2 assemblages, relative differences in assemblages between stations for each size class were comparable.

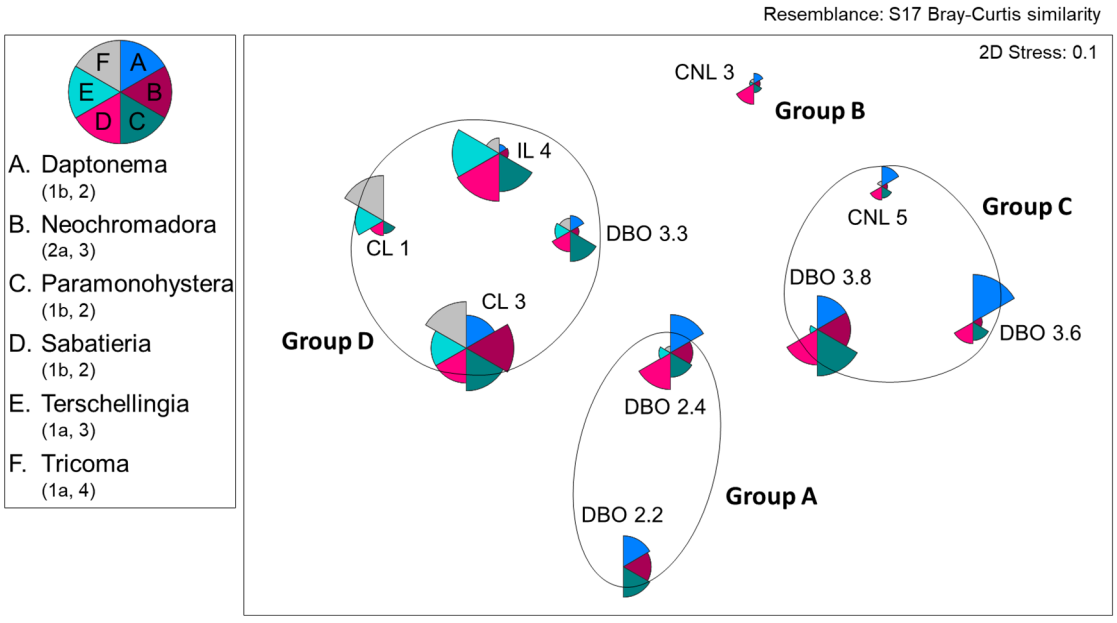

Fig. 6. nMDS ordination for community structure of meiofaunal-sized (63–500 µm) nematodes in surface (0–1 cm) sediments based on abundance data (ind. 10 cm^{-2}). Ordination based on hierarchical agglomerative clustering with group-averaged linkage on log(x + 1) transformed data and Bray-Curtis similarity. Four significant station groupings, circled in black or as a singleton station, are based on the similarity profile test. Pie slices represent the abundance of nematode genera that were in the top 3 guilds contributing to within-group similarity in at least 1 group based on similarity percentages procedure. Feeding type and c–p score of genera in parentheses

The most abundant macrofaunal-sized nematode genus at most stations was either *Paramonohystera* or *Sabatieria*, except at Stns DBO2.2 (*Cephalanticoma* and *Mesacanthion*) and CL1 (*Setosabatiera*; Table S7). *Paramonohystera* was generally dominant at northern stations, while *Sabatieria* was dominant at the southern Chukchi Sea stations and DBO2.4 (Table 2; Table S7).

Of the 67 genera recovered in the meiofaunal size fraction, 45 were not found in the larger fraction, including *Neochromadora* and *Tricoma*, which, along with other abundant genera, contributed to dissimilarity between the 2 size fractions. Ten genera were only found in the >500 µm size fraction, including *Ledovitia*, *Mesacanthion*, *Symplocostoma*, and *Thalassoalaimus*, and were mainly predators/scavengers (2B) or had high c–p scores (3 or 4).

Trophic diversity of the macrofaunal nematodes was lower than that of the meiofaunal nematode assemblages at all stations except CNL5 (Table S4). Nonetheless, as with the meiofaunal size fraction, non-selective deposit feeders (1B) were the dominant feeding type except at DBO2.2, where predators/scavengers dominated (2B). Predators/scavengers were also abundant north of the Bering Strait (CNL3 and CNL5) and at DBO3.3. At many sites, especially in Group D, the maturity index was lower in the macrofaunal size fraction than the smaller size fraction (Table S4), attributed to the high relative abundance of general opportunists (c–p score = 2), such as *Paramonohystera* and *Sabatieria*. Stn DBO2.2 also had a high abundance of c–p = 3 and 4.

4. DISCUSSION

This study is among the first meiobenthic studies in the Pacific Arctic. The most northern portion of our study area overlapped with that of Lin et al. (2014), which presented meiofaunal (>32 µm) abundance estimates (~1200 to 4900 ind. 10 cm^{-2}) down to 10 cm depth. These values were, on average, lower than our estimates of ~1500 to 12 000 ind. 10 cm^{-2} for the upper 5 cm, although variability among stations was similarly high. These differences may be due to temporal changes in meiofaunal standing stock during the 8 yr between sampling events, seasonal differences (June sampling versus July to September sampling), small-scale spatial variability, or regional differences. Although nematodes accounted for 96.6% of total meiofauna abundance at shallow stations, the taxonomic and functional diversity of nematodes was not assessed in this earlier work (Lin et al. 2014).

Further north in the northeast Chukchi Sea, meiofaunal abundance in surface sediments (0–1 cm) was between ~90 and 1300 ind. 10 cm^{-2}, with nematodes

Table 2. Relative abundance (%) and trophic category and maturity index (labeled in parentheses) of the most abundant (>1%) nematode genera per group (based on 0–1 cm sediment layer) for the (a) 63–500 µm and (b) >500 µm size fractions. Groups are based on hierarchical agglomerative clustering and similarity profile test of meiofaunal-sized nematode communities (Fig. 3). Genera highlighted in **bold** in (a) contributed >70% to within-group similarity based on a similarity percentages (SIMPER) procedure (note: Group B only contained 1 station, so a SIMPER analysis could not be performed for this group)

(a) 63–500 µm	Group A		Group B		Group C		Group D	
	(1b, 2) *Daptonema*	15.28	(1b, 2) *Sabatieria*	24.75	**(1b, 2) *Daptonema***	42.51	**(1a, 4) *Halalaimus***	19.18
	(2b, 4) *Oncholaimus*	11.65	(1b, 2) *Daptonema*	10.89	**(1b, 2) *Paramonohystera***	23.37	**(2a, 2) *Microlaimus***	11.05
	(1b, 1) *Monhystrella*	8.95	(2a, 3) *Marylynnia*	10.89	**(1b, 2) *Sabatieria***	12.67	**(1a, 4) *Tricoma***	8.24
	(1b, 2) *Paramonohystera*	7.67	(1b, 2) *Paramonohystera*	5.94	(2a, 3) *Neochromadora*	11.14	**(1b, 2) *Paramonohystera***	6.26
	(1a, 4) *Halalaimus*	6.55	(1b, 2) Comesomatidae	5.94	**(2a, 3) *Chromadorita***	3.24	(1b, 1) *Thalassomonhystera*	5.59
	(2a, 3) *Neochromadora*	6.46	(1a, 1) *Halomonhystera*	3.96	(1a, 4) *Halalaimus*	2.29	**(1a, 3) *Terschellingia***	4.79
	(2b, 3) *Viscosia*	5.61	(1b, 2) *Metalinhomoeus*	3.96			**(1b, 2) *Sabatieria***	4.49
	(1b, 2) *Sabatieria*	5.18	(1a, 4) *Halalaimus*	2.97			**(1b, 2) *Cervonema***	4.29
	(2a, 2) *Microlaimus*	4.43	(2a, 3) *Neochromadora*	2.97			**(1b, 3) *Campylaimus***	4.12
	(2a, 3) *Actinonema*	3.61	(1b, 1) *Monhystrella*	1.98			**(1a, 4) *Desmoscolex***	3.83
	(1b, 2) *Steineria*	2.70	(2a, 2) *Microlaimus*	1.98			(2a, 3) *Neochromadora*	3.49
	(2a, 3) *Trochamus*	2.70	(1b, 2) Xyalidae	1.98			**(2a, 3) *Aponema***	3.32
	(1a, 1) *Halomonhystera*	2.27	(2a, 3) Cyatholaimidae	1.98			(1b, 2) *Daptonema*	2.54
	(2a, 3) *Chromadorita*	2.15	(1a, 4) *Tricoma*	1.98			(1b, 2) *Eleutherolaimus*	2.00
	(1a, 3) *Diplopeltula*	1.88	(2a, 3) *Pseudomicrolaimus*	1.98			(2a, 2) *Desmodora*	1.79
	(1b, 1) *Thalassomonhystera*	1.33					(1a, 2) *Leptolaimus*	1.73
	(1a, 2) *Leptolaimus*	1.21					(1a, 3) *Diplopeltula*	1.73
							(2a, 3) *Chromadorita*	1.30
							(1a, 3) *Pselionema*	1.28
(b) >500 µm	Group A		Group B		Group C		Group D	
	Sabatieria	22.97	*Sabatieria*	62.07	*Paramonohystera*	67.70	*Paramonohystera*	32.62
	Cephalanticoma	17.15	*Marylynnia*	13.79	*Sabatieria*	19.85	*Sabatieria*	14.44
	Mesacanthion	12.28	*Metalinhomoeus*	6.90	*Halalaimus*	3.63	*Setosabatieria*	12.53
	Oncholaimus	9.95	*Viscosia*	6.90	*Daptonema*	2.91	*Mesacanthion*	9.92
	Daptonema	6.78	*Crenopharynx*	3.45	*Innocuonema*	1.49	*Oxyonchus*	9.92
	Oxyonchus	5.81	*Oncholaimus*	3.45	*Sphaerolaimus*	1.49	*Rhabdodemania*	5.84
	Metalinhomoeus	4.24	*Symplocostoma*	3.45	*Mesacanthion*	1.43	*Daptonema*	4.67
	Metoncholaimus	4.24					*Dorylaimopsis*	2.21
	Viscosia	4.17					*Thalassoalaimus*	1.24
	Ledovitia	3.30					*Metalinhomoeus*	1.17
	Paramonohystera	2.54						
	Steineria	2.45						
	Subsphaerolaimus	1.69						

Table 3. Hill's numbers (H_0, H_1, H_2, H_∞), Pielou's evenness (J'), Shannon-Wiener diversity index (H'), expected number of genera for 51 individuals (EG(51)), average trophic diversity (Heip et al. 1998), relative abundances of each feeding type, average maturity index (Bongers 1990, Bongers et al. 1991), and relative abundance of each c–p score for meiofaunal-sized (63–500 µm) nematodes in surface sediments (0–1 cm) for each group. Groups are based on hierarchical agglomerative clustering and similarity profile test (Fig. 3)

	Group A	Group B	Group C	Group D
H_0	26.5	31	12	26
H_1	15.0	16.9	5.0	15.5
H_2	10.3	9.9	3.4	10.1
H_∞	5.1	4.0	2.1	4.5
J'	0.83	0.82	0.62	0.84
H'	2.7	2.8	1.6	2.7
EG(51)	16.7	20.1	8.4	17.0
Trophic diversity	3.07 ± 0.69	2.42	1.53 ± 0.20	2.67 ± 0.22
Feeding type				
1A	15.3	12.9	3.3	43.2
1B	43.0	56.4	79.8	32.6
2A	23.3	27.7	15.9	23.7
2B	18.5	3.0	1.1	0.6
Maturity index	2.61 ± 0.20	2.41	2.25 ± 0.10	2.75 ± 0.24
c–p score				
2	52.9	66.3	80.7	46.3
3	26.2	26.7	16.0	22.0
4	20.9	6.9	3.3	31.8

accounting for 80.6 to 88% of meiofaunal abundance (Hajduk 2015). We observed higher abundances (351 to 7322 ind. 10 cm^{-2}) in the surface sediments. This study used the same sieve sizes; however, other methodological differences, including sample collection (multi-core versus van Veen grab) and extraction method (decantation versus Ludox centrifugation), may have influenced the differences in results.

4.1. Four spatially distinct assemblages of meiofaunal nematodes

Our study provides the first genus-level characterization and biomass estimates of nematodes in the northern Bering and southern Chukchi Seas. While no significant spatial patterns were detected in meiofauna at the phylum/class level nor for the macrofaunal-sized nematodes, patterns emerged through higher-resolution analysis of the meiofaunal-sized nematodes identified to genus, demonstrating the value of nematode studies for elucidating ecological patterns. Previous studies have indeed shown that patterns of ecological impact are robust at the species and genus level but change at higher levels of taxonomic aggregation (Somerfield & Clarke 1995). We observed 4 distinct communities of meiofaunal nematodes, occupying different regions of the study area associated with distinct local environmental conditions. Our sampling strategy was not designed to capture small-scale variability, which very likely occurs at each sampling location, and is dependent on topographical variations and other abiotic differences, ecological interactions, and, in turn, the availability and quality of food sources. Regional coverage of sampling stations was also limited, and further spatial patterns may remain as-yet uncovered. The 4 distinct meiofaunal nematode assemblages closely match the spatial distribution of polychaete and microbial communities in the area (Charrier et al. 2023, Walker et al. 2023), suggesting these regional patterns are consistent over multiple components of the infauna. Studies from other locations have found similar relationships among infauna, in which components of the meiofauna and macrofauna follow similar spatial patterns, although likely in response to different environmental factors (Baldrighi & Manini 2015, Gunton et al. 2017). In our

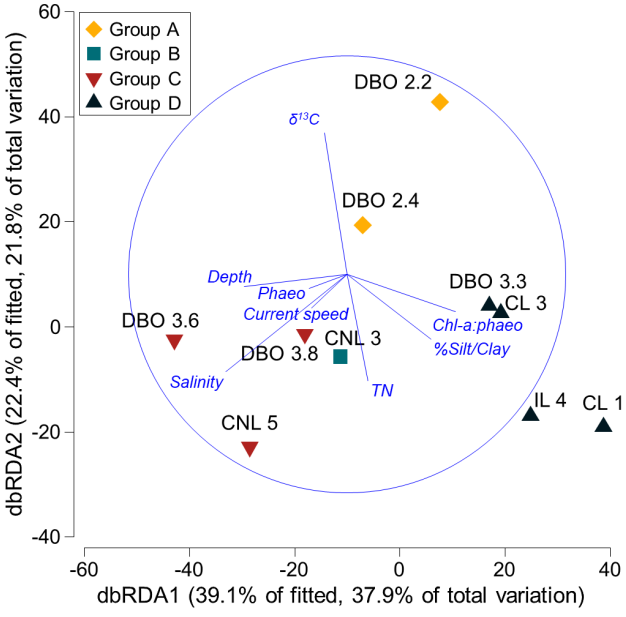

Fig. 7. Distance-based redundancy analysis (dbRDA) displaying the relationship between nematode (63–500 µm) community structure for the upper 1 cm of sediment and environmental correlates. The first 2 axes accounted for 59.7% of total variation, while the entire model (see Table S5) accounted for 96.97% of total variation

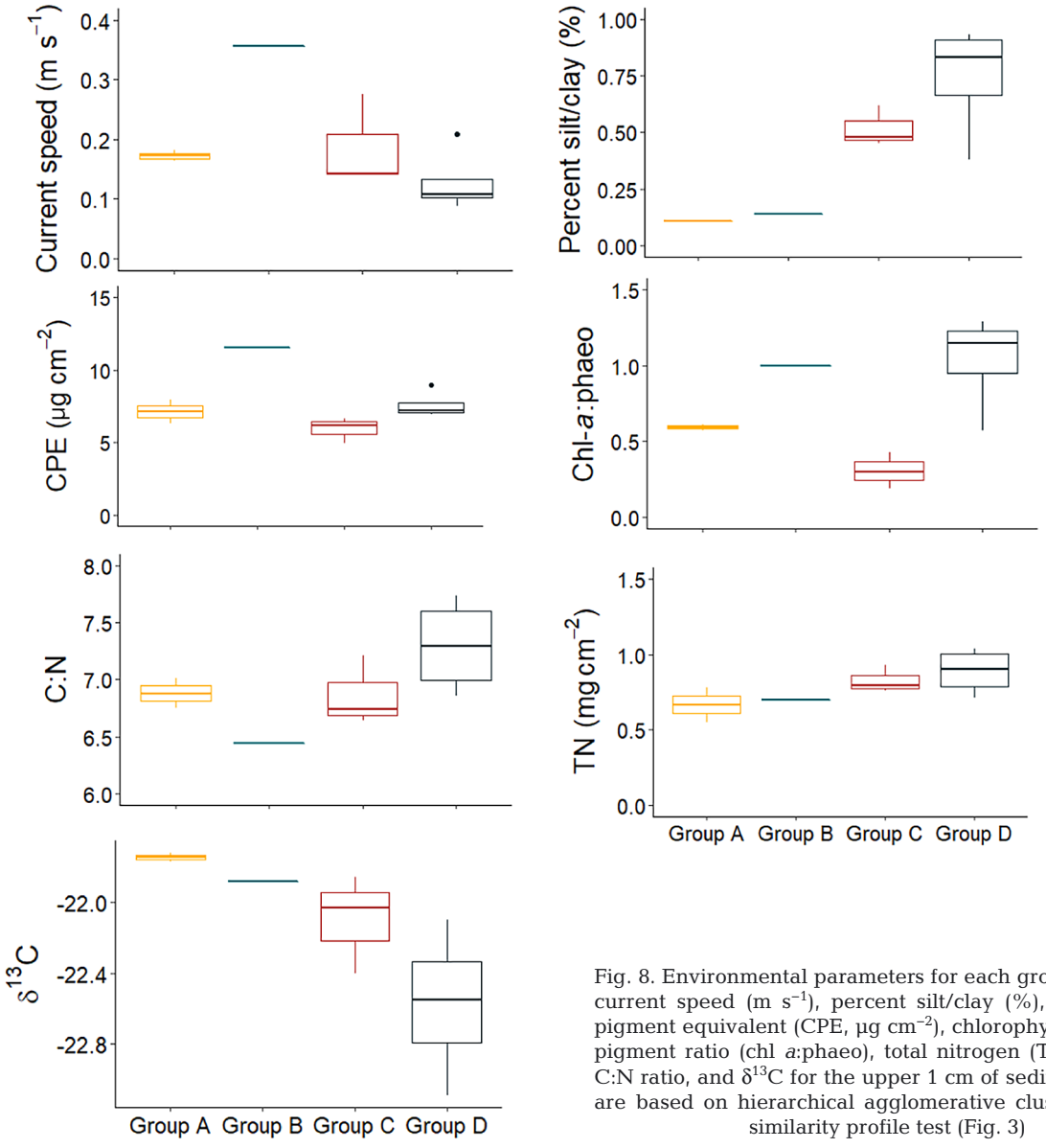

Fig. 8. Environmental parameters for each group, including current speed (m s^{-1}), percent silt/clay (%), chloroplastic pigment equivalent (CPE, µg cm^{-2}), chlorophyll *a* to phaeopigment ratio (chl *a*:phaeo), total nitrogen (TN, mg cm^{-2}), C:N ratio, and $\delta^{13}C$ for the upper 1 cm of sediment. Groups are based on hierarchical agglomerative clustering and a similarity profile test (Fig. 3)

study region, the polychaetes were more strongly correlated with total OM, while the meiofaunal assemblages were more closely associated with OM quality. Both were correlated with current speed and silt/clay content. Thus, while functional responses to abiotic conditions may differ among taxa in different size components of the benthos, the resulting spatial distinctions in assemblages that result from those responses are comparable among size components.

Considering the consistency in spatial patterns among these different benthic components, it is interesting that while spatial patterns between meio- and macrofaunal-sized nematode assemblages were related (i.e. both communities ranked the pairwise distances between sampling locations in a similar way), the macrofaunal nematodes did not exhibit the same significant spatial grouping pattern. The main reason for this inconsistency may be found in the functional composition of the macrofaunal nematode assemblages, dominated to a great extent by non-selective feeders, scavengers, and predators, and taxa with opportunistic life histories (low c–p scores). These larger taxa are characteristically less influenced by variable environmental conditions compared to meiofaunal nematode taxa. The meiofaunal nematode assemblages exhibited greater levels of niche selectivity (higher trophic diversity) and comprised taxa with more sensitive life histories (taxa with higher c–p scores and, therefore, assemblages with higher maturity index). These considerations

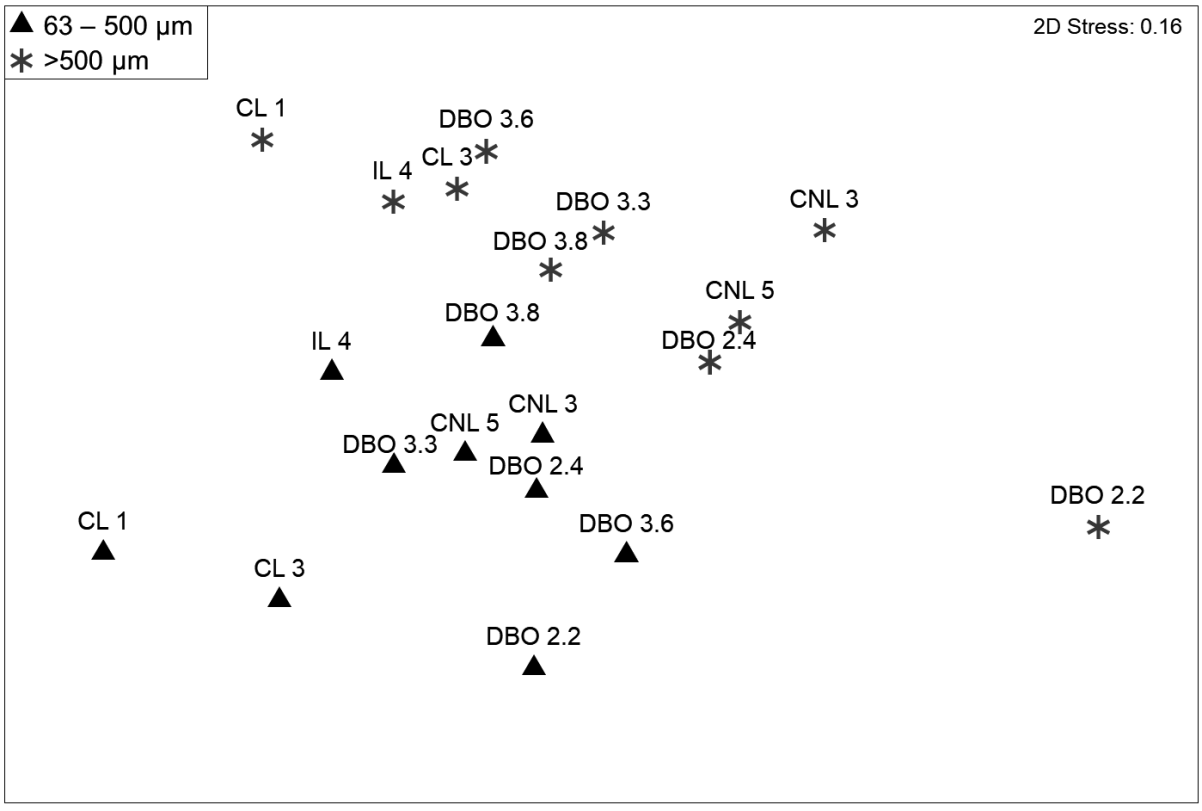

Fig. 9. nMDS ordination of meiofaunal- and macrofaunal-sized nematode relative abundance in surface sediment (0–1 cm). Ordination based on hierarchical agglomerative clustering with group-averaged linkage on log(x + 1) transformed relative abundances and Bray-Curtis similarity. The 2 size fractions were significantly different (ANOSIM R = 0.36, p = 0.0002). Black triangles are 63–500 µm samples, and gray asterisks are >500 µm samples

are discussed in more detail in Section 4.3. The meiofaunal-sized nematode assemblages separated into 4 distinct groups supported by correlative relationships with environmental conditions:

Group A comprised the Bering shelf stations (DBO2.2 and DBO2.4) within the Chirikov Basin, characterized by sandy sediment and low amounts of labile OM. The Chirikov Basin experiences moderate flow speeds, resulting in low sedimentation rates (Grebmeier 1993, Lovvorn et al. 2020). Notably in this group, the abundance of nauplii at DBO2.4 was nearly 5 times higher than at any other station, suggesting a recent recruitment event, potentially in response to a pulse of OM following the retreat of the sea-ice edge and subsequent spring bloom. The nematode assemblage in Group A showed high abundance, biomass, trophic diversity, and maturity index, indicative of a diverse community supported by a labile food source at the sediment surface or associated with suspended material. The high maturity index is a reflection in part of the high abundance of more persistent predators/scavengers in the assemblage (2B; e.g. *Oncholaimus* and *Viscosia*) in both the meiofaunal (18%) and macrofaunal (~30–55%) size fractions, which are likely supported by the high abundance of metazoan prey. However, while these sites had high abundance and biomass of relatively large-bodied taxa, most of the nematodes were concentrated in the upper 1 cm of sediment, and abundance declined rapidly with sediment depth (Fig. 4). This rapid decline in abundance may be due to low food availability below the surface layer of sediment in this advective system, likely supported by suspended material (Charrier et al. 2023). In food-poor environments, nematodes concentrate in surface sediments where food availability is higher (Lambshead et al. 1995, Górska et al. 2014) or exhibit a vertical migratory response to recent OM deposition to gain access to the newly deposited food. In the northeast Chukchi and Beaufort Seas, these genera and feeding types were also more abundant in sandy sediments similar to Group A sites (Mincks et al. 2021), suggesting an effect of substrate type. Large-bodied, motile nematodes are well adapted to move through sandy sediments. This pattern further suggests a generally food-limited habitat, where the fac-

ultative feeding strategy of the 2B group and their greater mobility are advantageous (Sharma & Bluhm 2010, Baldrighi & Manini 2015).

Group B comprised a single station (CNL3) immediately north of the Bering Strait. CNL3 and the station off the coast of Point Hope (DBO3.3; Group D) were the only sites with gravel (0.9 and 32%, respectively). These stations may experience hydrodynamic disturbance, such as scouring from strong currents, particularly at DBO3.3 where currents accelerate as they curve around Point Hope. Gravel may also indicate deposition of ice-rafted debris or ice scouring, which might occur at DBO3.3, where there was also a high proportion of silt/clay particles (38%). Stn CNL3 is influenced by the constriction of water masses moving through the Bering Strait and the deepening topography as the shallow Strait opens onto the Chukchi shelf. Such disturbances usually reduce meiofaunal abundance, as found in other hydrodynamically active areas such as canyons (Garcia et al. 2007, Ingels et al. 2013), and as observed here.

The nematode community composition and functional traits at CNL3 also indicate a disturbed environment. CNL3 was dominated by non-selective deposit feeders (56%) and general opportunists (c–p = 2), including *Sabatieria*, *Daptonema*, and *Paramonohystera*. *Sabatieria* was the most abundant genus at CNL3 (25%) and is often abundant in disturbed areas, hydrodynamically active sites, or sediments generally under stressed environmental conditions, such as low oxygen concentration (Ingels et al. 2011a,b, Mincks et al. 2021). The location downstream of the Bering Strait constriction, high current speeds, sandy and gravelly substrate, and the high abundance of *Sabatieria* support the hypothesis of a dynamic and disturbed environment at CNL3 due to strong currents. This disturbance is further supported by the high dominance of relatively few families of polychaetes, including the classic opportunist Capitellidae family (Charrier et al. 2023).

In the northeast Chukchi Sea, *Sabatieria* (37.6%) was the most abundant genus in the upper 1 cm of sediment, with the next 3 most abundant genera being *Daptonema* (10.7%), *Cervonema* (4.5%), and *Dorylaimoposis* (3.7%; Mincks et al. 2021). In our study, *Sabatieria* was the most abundant meiofaunal-sized nematode only in Group B, whereas *Daptonema* was highly abundant in Groups A, B, and C. *Cervonema* (CL1, CL3, IL4) and *Dorylaimopsis* (IL4) were found only in Group D, which included the northern coastal stations closest to the northeast Chukchi Sea study area. The variability in nematode genus composition suggests broader regional patterns that extend beyond our study area and point to the heterogeneous nature of Pacific-Arctic benthos.

Group C included 3 stations in the southern Chukchi Sea (CNL5, DBO3.8, and DBO3.6), with muddy sediment and low chloropigment content but high TOC and TN. Overall, these stations receive large inputs of OM (O'Daly et al. 2020, Feng et al. 2021), which result in high biomass of deposit-feeding macrofauna (Grebmeier et al. 2015) that may subduct this material through feeding activity and bioturbation. The meiofaunal and nematode community in Group C also reflects these large inputs of OM, with high meiofaunal abundance in the upper 5 cm of sediment, especially at DBO3.6 and DBO3.8, but also with subsurface abundance maxima (1–2, 2–3 cm). The nematode assemblages were dominated by non-selective deposit feeders (80%) and general opportunists (c–p = 2; 81%), including members of the Xyalidae family and *Sabatieria*, again pointing to an environment that experiences sedimentary disturbance. In contrast to the high meiofaunal abundance of small nematodes in Group C, total macrofaunal abundance was low at these stations (Charrier et al. 2023). However, macrofaunal biomass was high and dominated by a few species of large-bodied organisms, particularly bivalves. These bivalves can easily rework nutritious particles from the surface into subsurface sediment layers where nematodes may aggregate to exploit the redistributed food sources.

Group D contained the 4 coastal Chukchi Sea stations, characterized by muddy sediment and low current speeds (except at DBO3.3, see discussion of Group B above) with high concentrations of TOC and TN and a visible layer of recently deposited phytodetritus at the sediment surface at some sites. However, this region is influenced by the Alaska Coastal Water, which is generally more nutrient-poor and less productive (Danielson et al. 2017, O'Daly et al. 2020). High C:N ratios and low $\delta^{13}C$ values in sediments suggest that these relatively large sediment OM pools are partly comprised of refractory terrestrial material or advected particles, which enter the benthic food web in this area (Feder et al. 2007, Iken et al. 2010, Zinkann et al. 2021). This large amount of OM supports high nematode abundance and biomass in surface sediments, with total meiofaunal abundance at least 1.7 times and up to nearly 9 times higher at Stn CL3 than at other stations. The assemblage at CL3 also comprised the smallest individuals on average.

The high number of small nematodes at CL3 may have been juveniles produced during a recent recruitment event, perhaps in response to the spring

bloom. The presence of juveniles, as opposed to small adults, seems even more likely, considering CL3 exhibited one of the highest MI values, suggesting high numbers of larger, more persistent taxa. An additional explanation, however, is the dominance of *Halalaimus* at CL3 (>26%), which are long but extremely thin nematodes with relatively low biomass. Therefore, even a high abundance of *Halalaimus* would not substantially increase the nematode biomass at this station, further supporting the interpretation of small or young individuals being present. Although other stations had higher sediment chl *a* and TOC values, a visible layer of phytodetritus was observed in some sediment cores collected at CL3, suggesting a recent depositional event. Food pulses are important in regulating nematode size distributions as food inputs can stimulate reproduction (e.g. Ingels et al. 2013). The Pacific Arctic is indeed characterized by large pulses of OM input to the seafloor associated with the release of ice algae during melting and a strong spring phytoplankton bloom (Leu et al. 2015, Moore et al. 2018). Small organisms, such as meiofauna, respond more rapidly to pulsed food inputs (Lovvorn et al. 2016). Nematodes can also actively influence spatial distribution by becoming entrained in resuspended material and then selectively settling in food-rich patches, such as freshly deposited phytodetritus (Lins et al. 2013, Mevenkamp et al. 2016)

The nematode and meiofauna communities at Group D stations were representative of assemblages commonly found in muddy locations with high OM. For instance, the most abundant genus was *Halalaimus*, a long, slender nematode that can occupy interstitial space in fine sediments (Sharma et al. 2011). The family Desmodoridae (e.g. *Desmodora* and *Molgolaimus*) was only found at these sites and was also most abundant at muddy stations in the Southern Ocean (Ingels et al. 2006). Kinorhynchs, which are generally restricted to muddy sediment with higher OM (Grzelak & Sørensen 2019, Landers et al. 2019), were unique to Group D and particularly abundant at the muddiest stations: CL1, CL3, and IL4. Overall, these taxa suggest that the muddy substrate and OM quantity at these stations drive community composition.

A high trophic diversity index was found for Group D, which may be related to a diversity of sediment OM types, including greater inputs of terrestrial material at these nearshore sites. Elevated trophic diversity has been documented in both meio- and macrofauna in areas with heterogeneous composition of OM, including mixtures of fresh and degraded material (reviewed by Campanyà-Llovet et al. 2017). Higher proportions of selective deposit feeders were also found in Group D, including *Halalaimus*, *Tricoma*, and *Terschellingia*. Of particular interest is the genus *Terschellingia*, which has been found in abundance in sulfidic, shallow-water habitats and is known to tolerate challenging biochemical conditions (Vanreusel et al. 2010). *Terschellingia* is most likely indicative of a shallow redox boundary at Group D sites, corresponding with evidence of a transition from an aerobic microbial community in the upper 1 cm of sediments at these same sites to an anaerobic community below (Walker et al. 2023).

4.2. Vertical distribution of meiofauna

Meiofaunal abundance generally declines with sediment depth; however, the steepness of the vertical gradient in abundance can vary. For instance, in the Fram Strait, upper-slope stations with high food availability exhibited a more gradual decrease in meiofaunal density with sediment depth compared to deeper stations with low food availability, where a more rapid decline was observed with sediment depth (Górska et al. 2014). Similar trends have been found at other continental slope and abyssal sites (Lambshead et al. 1995, Vanaverbeke et al. 1997). At our shallower shelf sites, meiofaunal abundance decreased slowly with sediment depth at the muddy, coastal Chukchi stations characterized by high OM (Group D) and more rapidly at the sandy Bering Sea stations with lower sediment OM content (Group A).

We found a subsurface peak in total meiofaunal abundance at 4 southern Chukchi Sea stations (Groups B and C; Fig. 4), 2 of which showed the same pattern for macrofaunal abundance (Charrier et al. 2023). Such patterns may result from surficial predation pressure (Soltwedel et al. 2003), subsurface peaks of food availability due to bioturbation (Galéron et al. 2001), or physical disturbance (Braeckman et al. 2011). At the Group B station, disturbance due to high current speeds may cause resuspension of surface-dwelling meiofauna, promoting deeper burrowing. In addition, all stations with the subsurface abundance peaks also had high biomass of deeper-burrowing bivalves, which may facilitate subduction of OM to depth through bioturbation activity, contributing to the subsurface distribution of nematodes. Experimental studies have shown aggregations of nematodes in subsurface sediment in the presence of both physical and biological surface mixing (Braeckman et al. 2011).

4.3. Ecological role of macrofaunal-sized nematodes in the sediment food web

Macrofaunal-sized nematodes are often ignored in both macro- and meiobenthic studies, yet they exhibit distinct taxonomic and functional diversity compared to meiofaunal nematode assemblages (Sharma et al. 2011, Baldrighi & Manini 2015, Gunton et al. 2017). Similarly, we found that the meiofaunal- and macrofaunal-sized nematodes represented 2 distinct communities. The macrofaunal nematodes in our study comprised relatively fewer selective deposit feeders (1A) and epistratum feeders (2A) and higher proportions of non-selective deposit feeders (1B) and predators/scavengers (2B) relative to meiofaunal nematodes. Genera that were exclusively found in the >500 µm assemblage were mainly predators/scavengers or persisters (c–p = 3 or 4), which tend to be larger and thus better represented in this size fraction (Sharma & Bluhm 2010, Baldrighi & Manini 2015, Gunton et al. 2017). Predators/scavengers were particularly abundant in sandier locations, likely because greater interstitial space is more accommodating to their larger size and greater mobility, and perhaps more importantly, because their facultative feeding behavior and higher mobility may be advantageous in more food-limited habitats (Sharma & Bluhm 2010, Baldrighi & Manini 2015).

These differences in feeding-group composition suggest distinct roles of meio- and macrofaunal nematode communities in benthic carbon cycling. Many of the smaller nematodes are selective feeders, targeting labile food particles such as fresh phytoplankton cells or bacteria. These nematodes likely depend more heavily on labile OM and would be sensitive to changes in food input (Lovvorn et al. 2016), such as a decline in deposition of fresh phytoplankton to the seafloor, which has been predicted for the region (Lee et al. 2013, Moore & Stabeno 2015). Indeed, a global synthesis of available data suggests that meiofauna are generally more sensitive to changes in the freshness of phytodetritus and concentration of labile materials, such as proteins and dietary lipids, than macro- or megafaunal benthos (Campanyà-Llovet et al. 2017). In contrast, non-selective deposit feeders that dominate the macrofaunal-sized nematode communities may be better equipped to consume more refractory or reworked material. These taxa may be buffered against declines in the input of fresh phytodetritus to the seafloor through consumption of a sediment food bank of OM (Mincks et al. 2005, Pirtle-Levy et al. 2009). The larger predators/scavengers prevalent in macrofaunal-sized nematode communities can consume other meiofaunal organisms or the juveniles and scavenged remains of macrofaunal organisms, adding a trophic pathway to sedimentary systems that goes unnoticed when the larger nematodes are ignored. These findings suggest that there is an important intermediary ecological niche being filled by macrofaunal-sized nematodes, organisms that still have an interstitial lifestyle but are arbitrarily classified as macrofauna based on the sieve size used to separate them.

In addition to representing a distinct taxonomic and functional assemblage, macrofaunal-sized nematodes contributed substantially to total infaunal abundance and biomass, and hence benthic carbon cycling. While they only represented 1.6% of total nematode abundance (16–110 ind. 10 cm^{-2} in the upper 5 cm of sediment; similar to values reported by Gunton et al. 2017), they accounted for 22% of total nematode biomass overall due to their large size, with a high of 55% at DBO3.3. Macrofaunal-sized nematodes were also highly abundant relative to the rest of the macrofauna, comprising an average of 82 ± 17% (ranging from 48% at DBO2.2 to 96% at DBO3.6 and DBO3.8) of total macrofaunal abundance and 1 ± 2% (ranging from 0.005% at CNL3 to 7% at IL4) of macrofaunal biomass in the upper 5 cm sediment (macrofaunal data from Charrier et al. 2023). In the surface 1 cm layer of sediment, the macrofaunal-sized nematodes contributed less to total macrofaunal abundance (49 ± 27%, ranging from 11% at CL3 to 87% at DBO3.6) but made up a larger portion of total macrofaunal biomass (3 ± 8%, ranging from 0.002% at CL3 to 26% at IL4).

The contribution of nematodes to total macrofaunal abundance in our samples is high compared to other studies. In the Whittard Canyon, nematodes only accounted for up to 15% of total macrofaunal abundance for the upper 5 cm of sediment (Gunton et al. 2017) and between 16 and 40% at deep-sea sites in the Mediterranean Sea (>300 µm for upper 20 cm; Baldrighi & Manini 2015). However, these studies counted nematodes in macrofaunal samples that were live sieved prior to preservation, while our samples were sieved after preservation. Sieving live reduces retention of many taxonomic groups of macrofauna, especially soft-bodied, motile polychaetes (Degraer et al. 2007). Indeed, nematode counts from our macrofaunal samples that were sieved live yielded estimates of only 28 ± 19% of total macrofaunal abundance, which is nevertheless a substantial contribution. This discrepancy highlights the well-known potential for methodological bias when comparing results among studies.

The abundance and biomass of macrofaunal-sized nematodes imply that they contribute substantially to carbon demand in the Pacific-Arctic benthos, particularly considering their potential for high rates of production given their relatively short generation times. We estimated benthic secondary production using equations from Brey (1989), based on average individual weights and population biomass measured here. Values of macrofaunal-sized nematode production ranged from 0.5 to 4 g C m^{-2} yr^{-1}, which was, on average, 3 ± 2% of total secondary production (meiofaunal-sized nematodes + macrofaunal-sized nematodes + plus macrofauna from Charrier et al. 2023), ranging from 0.3% at CNL3 to 7% at DBO3.6. At all but 2 stations with high disturbance, macrofaunal-sized nematodes contributed, on average, 3 to 4% of total secondary production, suggesting that their contribution to carbon consumption is consistent throughout the region and should be considered in most environmental settings. These secondary production estimates are based on biomass and body size and do not directly account for many factors (Brey 1989), such as generation time, lifespan, and other species-specific differences. The relatively short generation time of nematodes may result in much higher secondary production than estimated here.

Estimated production of meiofaunal-sized nematodes ranged from 5 to 28 g C m^{-2} yr^{-1}, which on average accounted for 29 ± 26% of total estimated production (ranging from 3% at CNL3 to 84% at IL4). Meiofaunal-sized nematode production accounted for 1 to 17% of carbon flux to the seafloor, according to regional flux measurements (O'Daly et al. 2020), and was highest in Group D followed by Group C. However, this estimate assumes that all nematodes directly consume deposited material and does not consider differences in consumption of detritus among feeding types. Modeling studies have estimated that predatory nematodes consume only about 20% detritus or bacteria and 80% other nematodes or fauna (van Oevelen et al. 2011). Given that predatory nematodes are rare at most stations (0–24%; average 5%), this feeding type does not substantially impact our secondary production estimates. While many other factors influence metabolism and production, such as temperature, oxygen concentration, and food availability (Brockington & Clarke 2001, Clarke & Fraser 2004, Braeckman et al. 2013), these rough estimates of secondary production demonstrate that nematodes likely contribute a substantial amount to benthic carbon consumption due to high abundances and rapid generation times.

4.4. Conclusions

To predict potential impacts of future environmental change (Baker et al. 2020b, Huntington et al. 2020) on benthic ecosystem structure (Grebmeier 2012, Moore et al. 2018, Goethel et al. 2019, Waga et al. 2020) and function (Jones et al. 2021), ecosystem models must be well-constrained and representative of the current ecosystem and, where possible, consider the heterogeneity of the environment reflected by distinct communities of benthic organisms. So far, most benthic research in the Pacific Arctic has focused on the macro- or epibenthos (e.g. Bluhm et al. 2009, Grebmeier et al. 2015), even though meiofauna play critical roles in ecosystem functioning (reviewed by Schratzberger & Ingels 2018) and achieve high densities in other marginal ice zones (Hoste et al. 2007, Górska et al. 2014). Due to a lack of available data on meiofauna, modeling studies have utilized meiofaunal community metrics from other regions (Nelson et al. 2014, Lovvorn et al. 2016). Although the spatial coverage of our data and ability to assess small-scale heterogeneity are limited, our data begin to address some of these data gaps, specifically with nematodes. Our study shows 4 distinct nematode assemblages in the northern Bering and southern Chukchi Seas, providing a preliminary insight into the heterogeneous nature of the Pacific-Arctic sedimentary ecosystem, its distinct communities, and the environmental drivers that shape them. Moreover, the distribution of these assemblages aligns well with those of polychaete functional guilds (Charrier et al. 2023) and sediment microbes (Walker et al. 2023), reinforcing the distinctiveness of these 'eco-regions' and the strong environmental influence on biotic communities.

The data presented here fill important gaps, including nematode abundance, biomass, and community structure and function, that contribute to our understanding of ecosystem function. Our results suggest the need for small-scale, sub-regional ecosystem modeling units within the greater Pacific-Arctic region. Our research also shows that the size-based separation for infauna (meiofauna versus macrofauna) and the traditional taxonomic focus by scientists within each group leads to exclusion of a benthic component: the macrofaunal-sized nematodes. These nematodes can represent a substantial amount of benthic standing stock and play a distinct trophic role, yet are distinguished from taxa traditionally considered macrofauna. One can question whether the ecological niche occupied by macrofaunal-sized nematodes bridges those of meiofauna and macrofauna sensu stricto? Although they are meio-

faunal species and have many meiofaunal characteristics, the macrofaunal-sized nematodes fall within the upper bimodal size distribution typical of macrofauna (Warwick 1984, 2014). In addition to body size alone, we found that the meiofaunal- versus macrofaunal-sized nematodes are also distinguished by the meiofauna–macrofauna dichotomy of some functional traits, such as particle feeding discrimination (Warwick 1984, 2014), with the meiofaunal-sized nematodes displaying greater particle discrimination (higher proportion of selective deposit and epistratum feeders) and macrofaunal-sized nematodes characterized by more indiscriminate and opportunistic feeding (higher portion of non-selective deposit feeders and predators/scavengers). Overall, future field, experimental, and modeling studies should consider the potential bias when excluding macrofaunal-sized nematodes and assess their contribution to benthic ecosystem diversity and function.

Acknowledgements. This research was part of the North Pacific Research Board (NPRB) Arctic Integrated Ecosystem Research Program (Arctic IERP; www.nprb.org/arctic-program/). This manuscript is NPRB Publication ArcticIERP-47. Funding for the program was provided by the North Pacific Research Board, US Bureau of Ocean and Energy Management, Collaborative Alaskan Arctic Studies Program, and US Office of Naval Research. Generous in-kind support for the program was contributed by the US National Oceanic Atmospheric Administration Alaska Fisheries Science Center and Pacific Marine Environmental Laboratory, University of Alaska Fairbanks, US Fish and Wildlife Service, and US National Science Foundation. Funding was also provided by the North Pacific Research Board Graduate Student Research Award and the University of Alaska Dissertation Completion Fellowship. We thank the Captain and crew of the RV 'Sikuliaq' for making sampling possible and Opik Ahkinga, Silvana Gonzalez, and Andrew Thurber for help with sample collection. We also thank Tibor Dorsaz and Alexis Walker for lab assistance, Timothy Howe and others at the Alaska Stable Isotope Facility, and Amanda Kelly and Andrew Thurber for their valuable input and guidance. We are grateful to 3 anonymous reviewers for their constructive comments that helped improve earlier versions of this manuscript.

LITERATURE CITED

Anderson MJ, Gorley RN, Clarke KR (2008) PERMANOVA+ for PRIMER: guide to software and statistical methods. PRIMER-E, Plymouth

Andrassy I (1956) The determination of volume and weight of nematodes. Acta Zool 2:1–15

Arar EJ, Collins GB (1997) *In vitro* determination of chlorophyll *a* and pheophytin *a* in marine and freshwater algae by fluorescence. National Exposure Research Laboratory, Office of Research and Development, US Environmental Protection Agency, Cincinnati, OH

Baker MR, Farley EV, Ladd C, Danielson SL, Stafford KM, Huntington HP, Dickson DMS (2020a) Integrated ecosystem research in the Pacific Arctic — understanding ecosystem processes, timing and change. Deep Sea Res II 177:104850

Baker MR, Kivva KK, Pisareva MN, Watson JT, Selivanova J (2020b) Shifts in the physical environment in the Pacific Arctic and implications for ecological timing and conditions. Deep Sea Res II 177:104802

Baker MR, Farley EV, Danielson SL, Mordy C, Stafford KM, Dickson DMS (2023) Integrated research in the Arctic – ecosystem linkages and shifts in the northern Bering Sea and eastern and western Chukchi Sea. Deep Sea Res II 208:105251

Baldrighi E, Manini E (2015) Deep-sea meiofauna and macrofauna diversity and functional diversity: are they related? Mar Biodivers 45:469–488

Belicka LL, Harvey HR (2009) The sequestration of terrestrial organic carbon in Arctic Ocean sediments: a comparison of methods and implications for regional carbon budgets. Geochim Cosmochim Acta 73:6231–6248

Bell LE, Bluhm BA, Iken K (2016) Influence of terrestrial organic matter in marine food webs of the Beaufort Sea shelf and slope. Mar Ecol Prog Ser 550:1–24

Bezerra TN, Eisendle U, Hodda M, Holovachov O and others (2021) Nemys: World database of nematodes. http://nemys.ugent.be

Blott SJ (2010) GRADISTAT Version 8.0: a grain size distribution and statistics package for the analysis of unconsolidated sediments by sieving or laser granulometer. Kenneth Pye Associates, Crowthorne

Blott SJ, Pye K (2001) Gradistat: a grain size distribution and statistics package for the analysis of unconsolidated sediments. Earth Surf Process Landf 26:1237–1248

Bluhm BA, Iken K, Mincks Hardy S, Sirenko BI, Holladay BA (2009) Community structure of epibenthic megafauna in the Chukchi Sea. Aquat Biol 7:269–293

Bonaglia S, Nascimento FJA, Bartoli M, Klawonn I, Brüchert V (2014) Meiofauna increases bacterial denitrification in marine sediments. Nat Commun 5:5133

Bongers T (1990) The maturity index: an ecological measure of environmental disturbance based on nematode species composition. Oecologia 83:14–19

Bongers T, Alkemade R, Yeates GW (1991) Interpretation of disturbance-induced maturity decrease in marine nematode assemblages by means of the Maturity Index. Mar Ecol Prog Ser 76:135–142

Bongers T, de Goede RG, Korthals GW, Yeates G (1995) Proposed changes of c–p classification for nematodes. Russ J Nematol 3:61–62

Braeckman U, Provoost P, Moens T, Soetaert K, Middelburg JJ, Vincx M, Vanaverbeke J (2011) Biological vs. physical mixing effects on benthic food web dynamics. PLOS ONE 6:e18078

Braeckman U, Vanaverbeke J, Vincx M, van Oevelen D, Soetaert K (2013) Meiofauna metabolism in suboxic sediments: currently overestimated. PLOS ONE 8:e59289

Brey T (1989) Estimating productivity of macrobenthic invertebrates from biomass and mean individual weight. Meeresforschung Rep Mar Res 32:329–343

Brockington S, Clarke A (2001) The relative influence of temperature and food on the metabolism of a marine invertebrate. J Exp Mar Biol Ecol 258:87–99

Campanyà-Llovet N, Snelgrove PVR, Parrish CC (2017) Rethinking the importance of food quality in marine benthic food webs. Prog Oceanogr 156:240–251

Charrier BR, Danielson SL, Mincks SL (2023) Trait-based assessment of polychaete assemblages distinguishes macrofaunal community structure among four distinct benthic eco-regions on a shallow arctic shelf. Deep Sea Res II 208:105240

Clarke A, Fraser KPP (2004) Why does metabolism scale with temperature? Funct Ecol 18:243–251

Clarke KR, Gorley RN (2015) PRIMER v7: user manual/tutorial. PRIMER-E, Plymouth

Coull BC (1990) Are members of the meiofauna food for higher trophic levels? Trans Am Microsc Soc 109: 233–246

Coull BC (1999) Role of meiofauna in estuarine soft-bottom habitats. Austral Ecol 24:327–343

Creer S, Fonseca VG, Porazinksa DL, Giblin-Davis RM and others (2010) Ultrasequencing of the meiofaunal biosphere: practice, pitfalls and promises. Mol Ecol 19: 4–20

Curchitser E, Hedstrom K, Danielson SL, Kasper J (2018) Beaufort Sea Circulation Model Integrations. Final Report. OCS Study BOEM 2013-202. US Dept. of the Interior, Bureau of Ocean and Energy Management, Environmental Studies Program, Herndon, VA

Danielson SL, Eisner L, Ladd C, Mordy C, Sousa L, Weingartner TJ (2017) A comparison between late summer 2012 and 2013 water masses, macronutrients, and phytoplankton standing crops in the northern Bering and Chukchi Seas. Deep Sea Res II 135:7–26

Danielson SL, Hennon TD, Hedstrom KS, Pnyushkov AV and others (2020) Oceanic routing of wind-sourced energy along the Arctic Continental Shelves. Front Mar Sci 7:509

Degraer S, Moulaert I, Van Hoey G, Vincx M (2007) Sieving alive or after fixation: effects of sieving procedure on macrobenthic diversity, density and community structure. Helgol Mar Res 61:143–152

Feder HM, Jewett SC, Blanchard AL (2007) Southeastern Chukchi Sea (Alaska) macrobenthos. Polar Biol 30: 261–275

Feng Z, Ji R, Ashjian C, Zhang J, Campbell R, Grebmeier JM (2021) Benthic hotspots on the Northern Bering and Chukchi continental shelf: spatial variability in production regimes and environmental drivers. Prog Oceanogr 191:102497

Fonseca G, Soltwedel T, Vanreusel A, Lindegarth M (2010) Variation in nematode assemblages over multiple spatial scales and environmental conditions in Arctic deep seas. Prog Oceanogr 84:174–184

Galéron J, Sibuet M, Vanreusel A, Mackenzie K, Gooday A, Dinet A, Wolff G (2001) Temporal patterns among meiofauna and macrofauna taxa related to changes in sediment geochemistry at an abyssal NE Atlantic site. Prog Oceanogr 50:303–324

Garcia R, Koho KA, De Stigter HC, Epping E, Koning E, Thomsen L (2007) Distribution of meiobenthos in the Nazaré canyon and adjacent slope (western Iberian Margin) in relation to sedimentary composition. Mar Ecol Prog Ser 340:207–220

Gee JM (1989) An ecological and economic review of meiofauna as food for fish. Zool J Linn Soc 96:243–261

Giere O (2009) Meiobenthology: the microscopic motile fauna of aquatic sediments, 2nd edn. Springer-Verlag, Berlin

Goethel CL, Grebmeier JM, Cooper LW (2019) Changes in abundance and biomass of the bivalve *Macoma calcarea* in the northern Bering Sea and the southeastern Chukchi Sea from 1998 to 2014, tracked through dynamic factor analysis models. Deep Sea Res II 162:127–136

Górska B, Grzelak K, Kotwicki L, Hasemann C, Schewe I, Soltwedel T, Włodarska-Kowalczuk M (2014) Bathymetric variations in vertical distribution patterns of meiofauna in the surface sediments of the deep Arctic ocean (HAUSGARTEN, Fram strait). Deep Sea Res I 91:36–49

Gradinger R, Bluhm BA (2020) First analysis of an Arctic sea ice meiofauna food web based on abundance, biomass and stable isotope ratios. Mar Ecol Prog Ser 634:29–43

Grebmeier JM (1993) Studies of pelagic–benthic coupling extended onto the Soviet continental shelf in the northern Bering and Chukchi seas. Cont Shelf Res 13:653–668

Grebmeier JM (2012) Shifting patterns of life in the Pacific Arctic and Sub-Arctic Seas. Annu Rev Mar Sci 4:63–78

Grebmeier JM, Barry JP (1991) The influence of oceanographic processes on pelagic–benthic coupling in polar regions: a benthic perspective. J Mar Syst 2:495–518

Grebmeier JM, McRoy CP (1989) Pelagic–benthic coupling on the shelf of the northern Bering and Chukchi Seas. III. Benthic food supply and carbon cycling. Mar Ecol Prog Ser 53:79–91

Grebmeier JM, Bluhm BA, Cooper LW, Danielson SL and others (2015) Ecosystem characteristics and processes facilitating persistent macrobenthic biomass hotspots and associated benthivory in the Pacific Arctic. Prog Oceanogr 136:92–114

Grebmeier JM, Frey KE, Cooper LW, Kędra M (2018) Trends in benthic macrofaunal populations, seasonal sea ice persistence, and bottom water temperatures in the Bering Strait region. Oceanography 31:136–151

Grove SL, Probert PK, Berkenbusch K, Nodder SD (2006) Distribution of bathyal meiofauna in the region of the Subtropical Front, Chatham Rise, south-west Pacific. J Exp Mar Biol Ecol 330:342–355

Grzelak K, Sørensen MV (2019) Diversity and community structure of kinorhynchs around Svalbard: first insights into spatial patterns and environmental drivers. Zool Anz 282:31–43

Gunton LM, Bett BJ, Gooday AJ, Glover AG, Vanreusel A (2017) Macrofaunal nematodes of the deep Whittard Canyon (NE Atlantic): assemblage characteristics and comparison with polychaetes. Mar Ecol 38:e12408

Hajduk M (2015) Density and distribution of meiofauna in the northeastern Chukchi Sea. MSc thesis, University of Alaska Fairbanks, Fairbanks, AK

Heip C, Vincx M, Vranken G (1985) The ecology of marine nematodes. Oceanogr Mar Biol Annu Rev 23:399–489

Heip C, Herman PMJ, Soetaert K (1998) Indices of diversity and evenness. Oceanis 24:61–87

Higgins RP, Theil H (1988) Introduction to the study of meiofauna. Smithsonian Institution Press, Washington, DC

Hill MO (1973) Diversity and evenness: a unifying notation and its consequences. Ecology 54:427–432

Hoste E, Vanhove S, Schewe I, Soltwedel T, Vanreusel A (2007) Spatial and temporal variations in deep-sea meiofauna assemblages in the Marginal Ice Zone of the Arctic Ocean. Deep Sea Res I 54:109–129

Huntington HP, Danielson SL, Wiese FK, Baker M and others (2020) Evidence suggests potential transformation of the Pacific Arctic ecosystem is underway. Nat Clim Change 10:342–348

Iken K, Bluhm B, Dunton K (2010) Benthic food-web struc-

ture under differing water mass properties in the southern Chukchi Sea. Deep Sea Res II 57:71–85

Ingels J, Vanreusel A (2013) The importance of different spatial scales in determining structural and functional characteristics of deep-sea infauna communities. Biogeosciences 10:4547–4563

Ingels J, Vanhove S, De Mesel I, Vanreusel A (2006) The biodiversity and biogeography of the free-living nematode genera *Desmodora* and *Desmodorella* (family Desmodoridae) at both sides of the Scotia Arc. Polar Biol 29: 936–949

Ingels J, Billett DSM, Kiriakoulakis K, Wolff GA, Vanreusel A (2011a) Structural and functional diversity of Nematoda in relation with environmental variables in the Setú bal and Cascais canyons, Western Iberian Margin. Deep Sea Res II 58:2354–2368

Ingels J, Tchesunov AV, Vanreusel A (2011b) Meiofauna in the Gollum Channels and the Whittard Canyon, Celtic Margin—how local environmental conditions shape nematode structure and function. PLOS ONE 6:e20094

Ingels J, Vanreusel A, Romano C, Coenjaerts J, Mar Flexas M, Zúñiga D, Martin D (2013) Spatial and temporal infaunal dynamics of the Blanes submarine canyon-slope system (NW Mediterranean); changes in nematode standing stocks, feeding types and gender-life stage ratios. Prog Oceanogr 118:159–174

Jensen P (1984) Measuring carbon content in nematodes. Helgol Meeresunters 38:83–86

Jones BR, Kelley AL, Mincks SL (2021) Changes to benthic community structure may impact organic matter consumption on Pacific Arctic shelves. Conserv Physiol 9: coab007

Kennedy AD (1994) Carbon partitioning within meiobenthic nematode communities in the Exe Estuary, UK. Mar Ecol Prog Ser 105:71–78

Lambshead PJD, Ferrero TJ, Wollf GA (1995) Comparison of the vertical distribution of nematodes from two contrasting abyssal sites in the Northeast Atlantic subject to different seasonal inputs of phytodetritus. Int Rev Gesamten Hydrobiol Hydrogr 80:327–331

Landers SC, Sørensen MV, Sánchez N, Beaton KR, Miller JM, Ingels J (2019) Kinorhynch communities on the Louisiana continental shelf. Proc Biol Soc Wash 132:1–14

Lee SH, Yun MS, Kim BK, Saitoh S, Kang CK, Kang SH, Whitledge T (2013) Latitudinal carbon productivity in the Bering and Chukchi Seas during the summer in 2007. Cont Shelf Res 59:28–36

Leu E, Mundy CJ, Assmy P, Campbell K and others (2015) Arctic spring awakening - steering principles behind the phenology of vernal ice algal blooms. Prog Oceanogr 139:151–170

Lin R, Huang D, Guo Y, Chang Y, Cao Y, Wang J (2014) Abundance and distribution of meiofauna in the Chukchi Sea. Acta Oceanol Sin 33:90–94

Lins L, Vanreusel A, van Campenhout J, Ingels J (2013) Selective settlement of deep-sea canyon nematodes after resuspension — an experimental approach. J Exp Mar Biol Ecol 441:110–116

Lovvorn JR, North CA, Kolts JM, Grebmeier JM, Cooper LW, Cui X (2016) Projecting the effects of climate-driven changes in organic matter supply on benthic food webs in the northern Bering Sea. Mar Ecol Prog Ser 548:11–30

Lovvorn JR, Rocha AR, Danielson SL, Cooper LW, Grebmeier JM, Hedstrom KS (2020) Predicting sediment organic carbon and related food web types from a physical oceanographic model on a subarctic shelf. Mar Ecol Prog Ser 633:37–54

Mäkelä A, Witte U, Archambault P (2018) Short-term processing of ice algal- and phytoplankton-derived carbon by Artic benthic communities revealed through isotope labelling experiments. Mar Ecol Prog Ser 600:21–39

Mevenkamp L, Van Campenhout J, Vanreusel A (2016) Experimental evidence for selective settlement of meiofauna from two distinct environments after sediment suspension. J Exp Mar Biol Ecol 474:195–203

Mincks SL, Smith CR, DeMaster DJ (2005) Persistence of labile organic matter and microbial biomass in Antarctic shelf sediments: evidence of a sediment 'food bank.'. Mar Ecol Prog Ser 300:3–19

Mincks SL, Pereira TJ, Sharma J, Blanchard AL, Bik HM (2021) Composition of marine nematode communities across broad longitudinal and bathymetric gradients in the Northeast Chukchi and Beaufort Seas. Polar Biol 44: 85–103

Moore SE, Stabeno PJ (2015) Synthesis of Arctic Research (SOAR) in marine ecosystems of the Pacific Arctic. Prog Oceanogr 136:1–11

Moore SE, Stabeno PJ, Grebmeier JM, Okkonen SR (2018) The Arctic Marine Pulses Model: linking annual oceanographic processes to contiguous ecological domains in the Pacific Arctic. Deep Sea Res II 152:8–21

Nelson RJ, Ashjian CJ, Bluhm BA, Conlan KE and others (2014) Biodiversity and biogeography of the lower trophic taxa of the Pacific Arctic region: sensitivities to climate change. In: Grebmeier JM, Maslowski W (eds) The Pacific Arctic Region: ecosystem status and trends in a rapidly changing environment. Springer Netherlands, Dordrecht, p 269–336

North CA, Lovvorn JR, Kolts JM, Brooks ML, Cooper LW, Grebmeier JM (2014) Deposit-feeder diets in the Bering Sea: potential effects of climatic loss of sea ice-related microalgal blooms. Ecol Appl 24:1525–1542

O'Daly SH, Danielson SL, Hardy SM, Hopcroft RR, Lalande C, Stockwell DA, McDonnell AMP (2020) Extraordinary carbon fluxes on the shallow Pacific Arctic shelf during a remarkably warm and low sea ice period. Front Mar Sci 7:548931

Pape E, van Oevelen D, Moodley L, Soetaert K, Vanreusel A (2013) Nematode feeding strategies and the fate of dissolved organic matter carbon in different deep-sea sedimentary environments. Deep Sea Res I 80:94–110

Pirtle-Levy R, Grebmeier JM, Cooper LW, Larsen IL (2009) Chlorophyll *a* in Arctic sediments implies long persistence of algal pigments. Deep Sea Res II 56:1326–1338

Platt H, Warwick R (1988) Free-living marine nematodes. II. British chromadorids: pictorial key to world genera and notes for the identification of British species. EJ Brill, Backhuys, Leiden

Ridall A, Ingels J (2021) Suitability of free-living marine nematodes as bioindicators: status and future considerations. Front Mar Sci 8:685327

Román S, Vanreusel A, Ingels J, Martin D (2018) Nematode community zonation in response to environmental drivers in Blanes Canyon (NW Mediterranean). J Exp Mar Biol Ecol 502:111–128

Rysgaard S, Christensen PB, Sørensen MV, Funch P, Berg P (2000) Marine meiofauna, carbon and nitrogen mineralization in sandy and soft sediments of Disko Bay, West Greenland. Aquat Microb Ecol 21:59–71

Sajan S, Joydas TV, Damodaran R (2010) Meiofauna of the western continental shelf of India, Arabian Sea. Estuar Coast Shelf Sci 86:665–674

Schratzberger M, Ingels J (2018) Meiofauna matters: the roles of meiofauna in benthic ecosystems. J Exp Mar Biol Ecol 502:12–25

Seinhorst J (1959) A rapid method for the transfer of nematodes from fixation to anhydrous glycerin. Nematologica 4:67–69

Sharma J, Bluhm BA (2010) Diversity of larger free-living nematodes from macrobenthos (>250 µm) in the Arctic deep-sea Canada Basin. Mar Biodivers 41:455–465

Sharma J, Baguley J, Bluhm BA, Rowe G (2011) Do meio- and macrobenthic nematodes differ in community composition and body weight trends with depth? PLOS ONE 6:e14491

Soetaert K, Heip C (1990) Sample-size dependence of diversity indices and the determination of sufficient sample size in a high-diversity deep-sea environment. Mar Ecol Prog Ser 59:305–307

Soltwedel T, Wegener A, Miljutina M, Thistle D (2003) The meiobenthos of the Molloy Deep (5600 m), Fram Strait, Arctic Ocean. Vie Milieu 53:1–13

Somerfield PJ, Clarke KR (1995) Taxonomic levels, in marine community studies, revisited. Mar Ecol Prog Ser 127: 113–119

Somerfield PJ, Warwick RM (1996) Meiofauna in marine pollution monitoring programmes: a laboratory manual. MAFF Directorate of Fisheries Research, Lowestoft

Somerfield PJ, Warwick RM (2013) Meiofauna techniques. In: Eleftheriou A (ed) Methods for the study of marine benthos. John Wiley & Sons, Hoboken, NJ, p 253–284

van Oevelen D, Bergmann M, Soetaert K, Bauerfeind E and others (2011) Carbon flows in the benthic food web at the deep-sea observatory HAUSGARTEN (Fram Strait). Deep Sea Res I 58:1069–1083

Vanaverbeke J, Soetaert K, Heip C, Vanreusel A (1997) The metazoan meiobenthos along the continental slope of the Goban Spur (NE Atlantic). J Sea Res 38:93–107

Vanreusel A, Fonseca G, Danovaro R, Da Silva MC and others (2010) The contribution of deep-sea macrohabitat heterogeneity to global nematode diversity. Mar Ecol 31: 6–20

Waga H, Hirawake T, Grebmeier JM (2020) Recent change in benthic macrofaunal community composition in relation to physical forcing in the Pacific Arctic. Polar Biol 43: 285–294

Walker AM, Leigh MB, Mincks SL (2023) Benthic bacteria and archaea in the North American Arctic reflect food supply regimes and impacts of coastal and riverine inputs. Deep Sea Res II 207:105224

Walsh JJ, McRoy CP, Coachman LK, Goering JJ and others (1989) Carbon and nitrogen cycling within the Bering/Chukchi Seas: source regions for organic matter effecting AOU demands of the Arctic Ocean. Prog Oceanogr 22:277–359

Warwick RM (1984) Species size distributions in marine benthic communities. Oecologia 61:32–41

Warwick RM (2014) Meiobenthos and macrobenthos are discrete entities and not artefacts of sampling a size continuum: Comment on Bett (2013). Mar Ecol Prog Ser 505: 295–298

Wieser W (1953) The relationship between the mouth cavity form, feeding habit and occurrence in free-living marine nematodes: an ecological–morphological study. Ark Zool 4:439–484

Yeates G, Ferris H, Moens T, van der Putten W (2009) The role of nematodes in ecosystems. In: Wilson MJ, Kakouli-Duarte T (eds) Nematodes as environmental indicators. CAB International, Cambridge, p 1–44

Zinkann AC, Wooller MJ, O'Brien D, Iken K (2021) Does feeding type matter? Contribution of organic matter sources to benthic invertebrates on the Arctic Chukchi Sea shelf. Food Webs 29:e00205

Editorial responsibility: Martin Solan, Southampton, UK
Reviewed by: A. W. Muthumbi and 3 anonymous referees

Submitted: June 23, 2022
Accepted: August 4, 2023
Proofs received from author(s): September 27, 2023